Mol. Cells *32*, 459-475, November 30, 2011
DOI/10.1007/s10059-011-0150-3

Molecules and Cells

Protein Disulfide Isomerase-2 of *Arabidopsis* Mediates Protein Folding and Localizes to Both the Secretory Pathway and Nucleus, Where It Interacts with Maternal Effect Embryo Arrest Factor

Eun Ju Cho, Christen Y.L. Yuen, Byung-Ho Kang[1], Christine A. Ondzighi[2], L. Andrew Staehelin[2], and David A. Christopher*

Protein disulfide isomerase (PDI) is a thiodisulfide oxidoreductase that catalyzes the formation, reduction and rearrangement of disulfide bonds in proteins of eukaryotes. The classical PDI has a signal peptide, two CXXC-containing thioredoxin catalytic sites (*a,a*'), two noncatalytic thioredoxin fold domains (*b,b*'), an acidic domain (*c*) and a C-terminal endoplasmic reticulum (ER) retention signal. Although PDI resides in the ER where it mediates the folding of nascent polypeptides of the secretory pathway, we recently showed that PDI5 of *Arabidopsis thaliana* chaperones and inhibits cysteine proteases during trafficking to vacuoles prior to programmed cell death of the endothelium in developing seeds. Here we describe *Arabidopsis* PDI2, which shares a primary structure similar to that of classical PDI. Recombinant PDI2 is imported into ER-derived microsomes and complements the *E. coli* protein-folding mutant, *dsbA*. PDI2 interacted with proteins in both the ER and nucleus, including ER-resident protein folding chaperone, BiP1, and nuclear embryo transcription factor, MEE8. The PDI2-MEE8 interaction was confirmed to occur *in vitro* and *in vivo*. Transient expression of PDI2-GFP fusions in mesophyll protoplasts resulted in labeling of the ER, nucleus and vacuole. PDI2 is expressed in multiple tissues, with relatively high expression in seeds and root tips. Immunoelectron microscopy with GFP- and PDI2-specific antisera on transgenic seeds (PDI2-GFP) and wild type roots demonstrated that PDI2 was found in the secretory pathway (ER, Golgi, vacuole, cell wall) and the nuclei. Our results indicate that PDI2 mediates protein folding in the ER and has new functional roles in the nucleus.

INTRODUCTION

The classical protein disulfide isomerase (PDI, EC 5.3.4.1) is an oxidoreductase that catalyzes the formation, reduction, and isomerization of disulfide bonds in nascent secretory proteins in the lumen of the endoplasmic reticulum (ER) (Frand and Kaiser, 1998; Tu et al., 2000). PDI properly folds its target proteins into conformations necessary for stability, catalytic activity, trafficking and interaction with other proteins (Aslund and Beckwith, 1999; Gruber et al., 2006). The classical PDI has an N-terminal signal peptide, two thioredoxin catalytic sites, CXXC (*a, a*'), two thioredoxin fold domains (*b, b*'), and a KDEL ER retention signal with a very acidic C-terminus (Kanai et al., 1998). The *c* domain of animal PDIs has been proposed to serve as low-affinity, high-capacity Ca^{2+} binding domain (Lucero and Kaminer, 1999). PDI utilizes the thioredoxin domains for catalysis, which places them in the superfamily of thioredoxin-like proteins (Motohashi et al., 2001). However, PDIs are several-fold larger than thioredoxins (Ferrari and Soling, 1999; Lu and Christopher, 2008) and have other functions in addition to protein folding.

In animals and yeast, PDIs act as chaperones by preventing proteins from aggregating (Ferrari and Soling, 1999; Lamberg et al., 1996; Lumb and Bulleid, 2002) and are key subunits in numeous enzyme complexes (John and Bulleid, 1994; Lamberg et al., 1996). PDIs are required for cell viability (Ferrari and Soling, 1999) and differentiation (Ohtani et al., 1993), ion uptake (Honscha et al., 1993), regulating transcription (Markus and Benezra, 1999) and are found in the nucleus, cytoplasm, ER, mitochondria, and extracellular milieu (Couet et al., 1996; Lahav et al., 2000; Rigobello et al., 2001; Turano et al., 2002; Wilson et al., 1998). Recently, human PDI was found to bind signal peptide peptidase and unfold target proteins, leading to their dislocation from the ER to the cytoplasm and degradation by the ubiquitin-proteasome system, which is a process known as ER-associated degradation (ERAD) (Lee et al., 2010).

In the *Arabidopsis thaliana* genome, there are either 22 (Houston et al., 2005) or 12 *PDI*-like genes (Lu and Christopher, 2008), depending on whether the more distantly related adeno-

Department of Molecular Biosciences and Bioengineering, University of Hawaii, USA, [1]Department of Microbiology and Cell Science, University of Florida, USA, [2]Department of Molecular, Cellular and Developmental Biology, University of Colorado, USA
*Correspondence: dchr@Hawaii.edu

Received July 19, 2011; revised August 13, 2011; accepted August 16, 2011; published online September 5, 2011

Keywords: chaperone, endoplasmic reticulum, nuclear factor, plant disulfide isomerase, protein folding

sine 5′-phosphosulfate-like and quiescin-sulfhydryl oxidase gene families are included. In plants, PDIs have been implicated in several biological processes, including the unfolded protein response (Lu and Christopher, 2008) and folding storage proteins during the biogenesis of protein bodies from the ER in the seed endosperm (Li and Larkins, 1996; Okita and Rogers, 1996; Shimoni et al., 1995). In rice seeds, a PDI prevents proglutelin and prolamin from aggregating by chaperoning their segregation in the ER lumen (Takemoto et al., 2002). The rice PDIL1-1 localizes to the ER lumen, and facilitates the oxidative folding of vacuole-targeted storage proteins, such as proglutelins and a-globulin (Onda et al., 2011). Other PDIs have been found in chloroplasts of plants (Lu and Christopher, 2006; Shimada et al., 2007) and unicellular algae (Kim and Mayfield, 1997), where they play roles in starch biogenesis (Lu and Christopher, 2006), chaperone and foldase (Shimada et al., 2007), and light-regulated translation of the *psbA* mRNA (Kim and Mayfield, 1997). The chloroplast PDI, CYO1, is involved in thylakoid biogenesis in cotyledons, but not leaves (Shimada et al., 2007). In *Coffea arabica*, a PDI isomerizes disulfide bonds to create circular knotted proteins called cyclotides (Gruber et al., 2007).

Clear differences in subcellular localization and function of PDI5 and PDI11 have recently been reported in *Arabidopsis.* PDI5 inhibits and chaperones cysteine proteases during trafficking from the ER to the Golgi apparatus and to vacuoles prior to programmed cell death of the endothelium in developing embryos (Ondzighi et al., 2008). Insertional inactivation of the PDI5 gene hastens the onset of programmed cell death in embryos, preventing seed development. Alternatively, PDI11 is a strict ER resident that assists embryo sac maturation and pollen tube direction (Wang et al., 2008), but proteins interacting with PDI11 have not yet been identified.

A thorough understanding of the roles of PDIs in plants requires identifying their interacting partners, determining their biochemical activity, and localizing them to the subcellular compartments in which they function. In this report, we have studied *Arabidopsis* PDI2, and have identified a new role and subcellular location for a plant PDI, that of interacting with a transcription factor in the nucleus. PDI2 was characterized in terms of protein-folding function, interacting proteins, gene expression, microsomal processing, and subcellular localization. PDI2 complemented the *E. coli* protein-folding mutant, *dsbA*, and interacted with ER protein folding chaperone, BiP, and nuclear transcription factor, MEE8. PDI2 localized to the secretory compartments and nucleus. Taken together, the results indicate that PDI2 mediates protein folding and has functional roles in both the ER and with MEE8 in the nucleus.

MATERIALS AND METHODS

Plant materials, growth conditions, *pdi2* mutant genotyping, and T-DNA mapping

Seeds from *Arabidopsis thaliana* ecotype Columbia (Col-0) wild-type and the SALK T-DNA insertion lines SALK_115574 (*pdi2-1*) and SALK_017090 (*pdi2-2*) (http://signal.salk.edu), were used for the experiments and provided by the *Arabidopsis* Biological Resource Center. Wild-type and homozygous *pdi2* mutant seeds were surface-sterilized and then grown on soil (Farfard Super Fine Germinating Mix, American Clay Works & Supply Company, USA) under 16 h-light/8 h-dark cycles at 22-25°C for 4-6 weeks, and on solid Murashige-Skoog (Phytotechnology Laboratories) media supplemented with 2% (w/v) sucrose and 0.8% (w/v) Gellan Gum (Sigma-Aldrich), each at a standard light intensity of 50-60 mol m^{-2} s^{-1}. The homozygous

Table 1. List of primers used in this research and referred to in the "Materials and Methods"

Primer	Sequence	Modifications
A	5′-TGGTTCACGTAGTGGGCCATCG-3′	
B	5′-GTTACTTGTTAGATCTCAACAACCAG-3′	
C	5′-ATGTAGTTAGATTATACACACCAGGACC-3’	
D	5′-ACTACCATGGCGTTCCGCGTTTTGCTC-3′	*Nco*I
E	5′-TTTCCATATGCAATTCGTCCTTCGAGTCAC-3′	*Nde*I
F	5′-TTGCAGGAGATGATGCTCCCAGG-3′	
G	5′-CATTCCCACAAACGAGGGCTGG-3′	
H	5′-TGCCACGGAGCTTAAGGAAGATGG-3′	
I	5′-ACACCATGGTGCGTAGACCTCG-3′	
J	5′-GTCGGATCCTATGGCGTTCCGCGTTTTGCTCC-3′	*Bam*HI
K	5′-GCGGTCGAC**GTGGTGGTGGTGGTGGTG**CAAT TCGTCCTTCGAGTCACTTT-3′	*Sal*I; 6xHis
L	5′-CACCGACTAGTCATATGGTGAGCAAGGGCGAG-3′	*Nde*I
M	5′-TACAGGGTCACCTTACTTGTACAGCTCGTCCAT G-3′	*Bst*EII
N	5′-AGGATGGTCACCTAAAGCTCATCTTTGCCGTGA GTGATC-3′	*Bst*EII; KDEL
O	5′-CTTAAAACTAGTAAAAGAATGAACAAGGAC-3′	*Spe*I
P	5′-CCAGGGATCCCATATTCCCTGCGAACC-3′	*Bam*HI

T-DNA lines were crossed with wild type-Col-0 and followed by four generations of selfing. The homozygosity and the position of the T-DNA insertion within the *PDI2* gene (accession No. At5g60640) for *pdi2-1* (SALK_115574) were verified by PCR analysis of genomic DNA using a T-DNA left border primer A, as well as gene-specific primers B and C (Table 1). Homozygous SALK_01709 plants (*pdi2-2*) were identified using gene-specific primers D and E. The accurate T-DNA insertion positions were determined by sequencing the PCR products obtained from primer combinations A + B and A + D (Table 1).

In vitro transcription/translation, microsomal processing

The *PDI2* cDNA was transcribed in vitro as a circular plasmid (1 mg) using the T3 promoter and then translated in the reticulocyte lysate containing [^{35}S] methionine with and without 2 ml canine pancreatic microsomal membranes according to the manufacturer (TNT kit; Promega, USA). The samples were incubated at 30°C for 0, 10, 30 and 60 min, then quenched on ice. Selected reactions were treated with 2 ml proteinase K (4 units, New England Biolabs, USA) or 1% Triton-X-100 and incubated 1 h at 15°C. Samples were mixed with an equal volume of 2× loading buffer and electrophoresed on a 10% resolving, 5% stacking SDS-PAGE gel (described above). After electrophoresis for 1 h at 60 V, then 2.0 h at 80 V in 1 × Tris-Glycine buffer, pH 8.3, the gel was vacuum dried at 80°C for 1 h and exposed to X-ray film O/N (Neuteboom et al., 2009).

RNA isolation, RT-PCR, cloning the *PDI2* cDNA and creation of mGFP4 fusions

Total RNA was isolated from *Arabidopsis* tissue with an RNeasy Plant Mini kit (Qiagen, USA). RNA concentration was determined spectrophotometrically and its integrity was verified using denaturing gel electrophoresis (Chun et al., 2001). For RT-PCR, the RNA was treated with RNase-free DNase (Promega Inc.,

USA) and used to produce the first-strand cDNA with M-MLV reverse transcriptase (Promega, USA). Then the first strand cDNA was used in PCR with the Bio-X-Act Short Mix (Bioline Inc., USA). Amplification of actin and *PDI2* cDNA was performed using primers F+G and H+I, respectively. The primers corresponded to exon-exon junctions to avoid amplification of genomic DNA. The PCR products were sequenced to confirm their sequence and identities. The *Arabidopsis PDI2* cDNA derived from RT-PCR (accession No. locus At5g60640) was cloned into pSK (Bluescript, Stratagene, USA) and pET25b(+) vectors (Novagen, USA).

The *mGFP4* gene was obtained from the commercial vector pBIN-*gfp4* (Haseloff et al., 1997) by restriction digestion. A 1398 bp *PDI2* promoter region was amplified by PCR. The sequence began at (5′-TGTCACGCATGTTTTAAATC-3′) and ended at (5′-CAACAACCAGGTCGCACACA-3′), residing 5 bp upstream from the *PDI2* initiator methionine. It was ligated to the first 1081 bp of the *PDI2* cDNA, encoding the first 360 residues of the N-terminal half of the PDI2 protein, and an MDEL ER retention-like sequence was at the C-terminus. This construct was fused in-frame at the C-terminus to the GFP4 gene using a 7 amino acid *Bam*HI linker in plasmid pCAMBIA1300. An ER retention-like MDEL sequence was present at the C-terminus of GFP4. The resulting plasmid was named, p1300-Pdi2Pr-Nter-BH-mGFP4 (abbreviated 2PB4). The plasmid was introduced into disarmed *Agrobacterium tumefaciens* strain LB4404 and used to transform *Arabidopsis* (Col-0) wild-type using the method for dipping of floral buds (Clough and Bent, 1998).

Sequence analysis, alignments and sorting predictions

DNA sequencing was conducted at the University of Hawaii Advanced Studies of Genomics, Proteomics and Bioinformatics (ASGPB) (http://asgpb.mhpcc.hawaii.edu/). Protein domains were identified using Pfam (Finn et al., 2006) against the classical PDI structure (Gruber et al., 2006) (http://www.ch.embnet.org/software/BOX_form.html). Polypeptide sequences were aligned using the Clustal-W alignment program (http://align.genome.jp/). Nuclear localization signals were predicted using the algorithm of Cokol et al. (2000) at (http://cubic.bioc.columbia.edu/services/predictNLS/) and signal peptides were identified with (http://www.cbs.dtu.dk/services/).

Antisera, protein extraction, SDS-PAGE, and immunoblot analysis

A polyclonal antiserum was raised against a unique synthetic peptide (New England Peptide, USA) corresponding to amino acid residues (KMFHLDPESKRPALV, residues 268-282) from within PDI2 (BAB09837). The antiserum was affinity-purified by the company using the unique PDI2 peptide column. The GFP antibody was purchased from Invitrogen Molecular Probes Co. (USA). Tissues were collected from 14 day-old wild-type plants grown on soil and MS-agar plates. Fresh tissue and frozen yeast pellets were homogenized in 10 mM HEPES, pH 7.5, 0.2 M sucrose, 2 mM EGTA, 5 mM MgCl, supplemented with protease inhibitor cocktail (Sigma-Aldrich, Inc., USA), and Triton X-100 to 0.5% (v/v). Following centrifugation (one min, 1,000 × *g*), the pellet was discarded, and protein concentrations in the Triton X-100 supernatant were determined (BioRad, Co., USA), using BSA as a standard.

Protein samples were incubated in buffer (2% SDS, 0.1 M DTT, 10% glycerol, 0.05 M Tris-HCl, pH 6.8) and separated with 10% (w/v) SDS-PAGE on polyacrylamide mini-gels (with the ratio of 1:29 for Bis to Acrylamide). After electrophoresis, gels were stained with Coomassie blue and air-dried on gel drying films (Promega, Inc., USA), or transferred to PROTRAN pure nitrocellulose membrane (PerkinElmer Life Sciences, USA) with a BioRad mini-transblot apparatus using transfer buffer (25 mM Tris-OH, pH 8.3, 190 mM glycine, 20% methanol). The blots were blocked for 1 h at RT with 5% non-fat milk (Carnation, Inc.) in 1X Tris-buffered saline (20 mM Tris-HCl, pH 7.5, 200 mM NaCl) containing 0.1% Tween 20. Protein blots were incubated with the polyclonal anti-PDI2 antiserum at 1:1000 dilution for 1 h at RT, and conjugates were detected using the ECL anti-rabbit IgG linked to horseradish peroxidase and the ECL™ chemiluminescence's kit (Amersham Biosciences, USA). Chemiluminescent and fluorescent signals (ethidium bromide from RT-PCR described above) were developed and quantitated using a Kodak IS4000MM Image Analysis Imaging System and Image Analysis Software version 3.5.

Complementation of the *E. coli dsbA* mutant and alkaline phosphatase assay

A full-length *PDI2* cDNA coding was amplified by PCR from *Arabidopsis* cDNA using primers J and K (Table 1), with an in-frame His-tag was incorporated into the latter. The PDI2 cDNA was ligated into the pFLAG-CTS™ expression vector (Sigma-Aldrich Corp., USA), and the correct sequence was verified by sequencing. The *E. coli dsbA* mutant (R190; *ΔaraBAD-714, [araD139], Δ(codb-lacI)3, phoR82, galK16, galE15(GalS), LAM-, el4-, relA1, rpsL150(strR)*, *spoT1, dsbA1::kan, mcrB1*) was obtained from the *E. Coli* Genetic Stock Center (New Haven, CT USA). The *dsbA* mutant, with and without the *PDI2* cDNA, and the *dsbA* mutant with the empty pFLAG vector, and wild type *E. coli* (DE31) were grown on M9 minimal medium at 37°C. The cell pellets were harvested by centrifugation at 3,000 × *g* for 10 min at 4°C, and were washed with Tris-OH (pH 8.0) for use in immunoblot analysis and the alkaline phosphatase assay. Expression of *PDI2* in *E. coli* was verified by immunoblot analysis, as described above, except 1% alkali-soluble casein was used as a blocking agent for the anti-HIS monoclonal antiserum (used at 1:1000 dilution; Novagen EMD Biosciences, USA). The Quanti-ChromTM Alkaline Phosphatase Assay kit (DALP-250) (BioAssay Sytems, USA) was used according to the manufacturer's instructions. Alkaline phosphatase activities in units (IU/L = μmol/(L·min) were measured at OD 405 nm using a microplate reader (Tecan Group Ltd., Switzerland), and were calculated according to the manufacturer.

Yeast two-hybrid analysis of the PDI2 protein

The coding cDNA for residues 21 through 497 of the 501 residues PDI2 protein (BAB09837) were inserted into the pBUTE vector (a kanamycin-resistant version of GAL4 bait vector pGBDUC1 (James et al., 1996) as a translational fusion to the GAL4 DNA-binding domain. The resulting PDI2 bait vector was sequenced to confirm an in-frame fusion, then transformed into mating type A of strain PJ694 and tested for autoactivation of the β-galactosidase reporter gene (lacZ), and then used in a yeast two-hybrid (Y2H) screen (Durfee et al., 1993; Fields and Song, 1989) of two *Arabidopsis* cDNA libraries cloned as fusions to the GAL4 activation domain in pGADT7-rec (Clontech). One library was prepared from 3-day-old etiolated seedlings, and the second was a composite prepared from entire 3-week-old seedlings stressed by various hormones, osmotic, and environmental treatments. Approximately 18 million clones were screened via mating at the University of Wisconsin-Madison Molecular Interaction Facility (www.biotech.wisc.edu/mif/). Putative interactors were identified by growth on histidine dropout medium plus 1 mM 3-amino-1,2,4-triazole and by β-galactosidase assays (described below). Negative controls included media only, empty prey (activation domain) vector (pGADC1;

James et al., 1996), prey construct expressing mouse epsin, prey construct expressing human Fbox5, whereas positive controls for the Y2H system were two pre-mated interacting pairs: EH:Epsin (Rosenthal et al., 1999). Following selection, 40 yeast wells tested positive (via selection on histidine drop-out plus 1 mM 3AT and β-galactosidase assay) for interaction. From these, 35 representative prey plasmids were re-transformed into the alpha mating type of PJ694 and validated in a parallel mating and selection assay with the PDI2 bait and the empty bait vector. Yeast were mated on yeast extract-peptone-dextrose medium plus adenine for 24 h at 30°C and then grown on complete supplemental medium (Q-BIOgene, USA) minus leucine and tryptophan. 15 clones were consistently positive (grew in interaction selection media and β-gal positive) in the validation test, all of which were identified via sequencing. Of the 15, 10 were unique, while 5 were identified as repeat multiple isolates (RD2, Syntaxin, MEE8). The β-galactosidase activity was assayed in uniform density yeast cultures (OD620) lysed by the addition of yeast protein extraction reagent (YPER, Pierce Biotechnology, USA) combined with chlorophenyl red-β-D-galactopyranoside (CPRG; Roche Diagnostics, Germany) as a substrate and color intensity measured in the spectrophotometer at OD550.

Co-immunoprecipitation of two-hybrid positive isolates with PDI2 antiserum

Protein extracts (400 μg of total protein) were derived from yeast co-transformants containing PDI2 in pBute vector plus one of the individual clones (36, 37, Bip, 39, 47, or 52; refer to Table 2) or empty pBute (negative control) in co-immunoprecipitation buffer (20 mM Tris-Cl, pH 8.0, 150 mM NaCl, 1 mM EDTA, 1 mM phenylmethylsulfonyl fluoride, 1 mM dithiothreitol) and protease inhibitor cocktail (Roche Diagnostics, USA). The extracts were incubated with anti-HA tag antibody O/N at 4°C, then 30 μl of Protein-A Agarose beads (Invitrogen, Inc., USA) were added and the mixture was rotated 40 rpm for 1 h at 4°C. The agarose beads were centrifuged at 3,000 × *g* for 10 min at 4°C, and washed three times with 500 μl 1X wash buffer (20 mM Tris-Cl, pH 8.0, 150 mM NaCl, 1 mM EDTA, 1 mM phenylmethylsulfonyl fluoride, 1 mM dithiothreitol, 1%[v/v] Triton X-100, and protease inhibitor cocktail). After removing traces of buffer from the pellet, it was resuspended in 25 μl of protein loading buffer, heated to 95°C for 5 min, and gently centrifuged for 30 s at 2,000 × *g*. Supernatants were loaded onto a 10% SDS polyacrylamide gels. As controls for no co-immunoprecipiation, 25 μg empty pBute vector, yeast PDI2 and Bip were separately loaded on the gel. The proteins were transferred to a nitrocellulose membrane and incubated with a 1:750 dilution of anti-PDI2 primary antibody (described above), followed by a 1:5000 dilution of anti-rabbit horseradish peroxidase-conjugated secondary antibody for chemiluminescence detection using the ECL kit (GE Healthcare, Inc.). For the Anti-HA immunoblot, proteins precipitated with the mouse monoclonal anti-HA antiserum were detected with a rabbit anti-HA antiserum.

Expression of PDI2-GFP(S65T) and sub-cellular marker-mCherry constructs in protoplasts and visualization by laser scanning confocal microscopy

PDI2 subcellular localization was studied using the *Arabidopsis* mesophyll protoplast transient expression system (Yoo et al., 2007). Protoplasts were isolated from the leaves of 2-4 week-old plants using the Tape-Sandwich method (Wu et al., 2009), and transfected with fluorescent reporter constructs. Following transfection, protoplasts were incubated at RT under constant darkness in W5 solution (154 mM NaCl, 125 mM $CaCl_2$, 5 mM KCl, 5 mM glucose, and 2 mM MES pH 5.7) for 12-24 h prior to examination with an Olympus Fluoview 1000 laser scanning confocal microscope. GFP(S65T) was detected by excitation at 488 nm and using a 505-525 nm emission filter, mCherry by excitation at 543 nm and using a 560-620 nm emission filter, and chloroplast autofluorescence by excitation at 633 nm and using a 650 emission filter.

Since PDI2 possesses the C-terminal ER-retention motif, KDEL, reporter constructs both with and without KDEL at the C-terminal end of GFP(S65T) were developed. Construct 35S:PDI2-GFP(S65T) was created by inserting the genomic DNA sequence of *PDI2* between the *Nco*I and *Nde*I sites, and the *GFP(S65T)* coding sequence between the *Nde*I and *Bst*EII sites, of plasmid 35S:CNGC10-EGFP (Christopher et al., 2007). The *PDI2* fragment was amplified from wildtype Col-0 genomic DNA with primers D and E. The *GFP(S65T)* fragment was amplified from plasmid HBT95::sGFP(S65T)-NOS with primers L and M. Construct 35S:PDI2-GFP(S65T)+KDEL was generated by replacing the *GFP(S65T)* fragment of 35S:*PDI2-GFP(S65T)* with a modified version of *GFP(S65T)*, amplified using primers L and N, which alters the C-terminus of the encoded product from MDELYK to KDEL.

Derivatives of the organelle markers developed by Nelson et al. (2007) were created. The expression cassettes of binary plasmids ER-rk (ABRC stock number CD3-959) and vac-rk (gamma-tonoplast intrinsic protein, TIP, CD3-975) were excised by digestion with enzymes *Sac*I and *Hin*dIII, and ligated between the corresponding restriction sites of bacterial cloning vector pBluescript KS(+). The new plasmids were designated as pBL[ER-r] and pBL[vac-r], respectively. Both encode for fluorescent protein fusions containing the monomeric RFP variant, mCherry. Construct 35S:MEE8-RFP was generated by amplifying the genomic DNA sequence of *Arabidopsis MEE8* (*At1g25310*) with primers O and P, and cloning the fragment between the *Spe*I and *Bam*HI sites of pBL[vac-r]. Note that this fusion was developed based upon the actual sequence of the *MEE8* cDNA clone obtained from our yeast two-hybrid screen, and contains a different intron-exon structure than the bioinformatic gene model prediction on the TAIR website, which contains a frameshift at the 3′ end relative to our *MEE8* cDNA clone, resulting in an earlier predicted stop codon. Fusions of our *MEE8* cDNA correctly localized to the nucleus. An alternate version *MEE8* fusion based on the TAIR gene model was also developed, but no fluorescence was detected when the construct was transiently expressed in protoplasts, indicating premature translational termination (data not shown).

FRET and acceptor photobleaching analysis

The transfected protoplasts were fixed for fluorescence resonance energy transfer (FRET) analysis. They were centrifuged at 1,000 rpm for 2 min and the supernatant was carefully removed and 1 ml of fixative with 4% formaldehyde in 1X MTSB (100 mM Pipes-KOH pH 6.9, 10 mM $MgSO_4$, 10 mM EGTA) was added. The protoplasts were fixed for 1 h at RT, and then centrifuged at 1,000 rpm for 2 min and washed three times with 1 ml of 1X MTSB. The fixed protoplasts were pipetted in a 7 μl volume on a microscope slide and then dried in the hood for 5 min. The 5 μl of VECTASHIELD Mounting Medium (Vector Labs, Inc., USA) was added to each sample and then the edges of the cover slip were sealed with clear nail polish. The transfected protoplasts were imaged using a Leica TCS SP5 laser scanning confocal microscope (Buffalo Grove, USA). FRET analysis was performed with the Acceptor Photobleaching FRET wizard module of the Leica AF program package. As a negative control for FRET, the nuclear protein PSAT6::mCherry

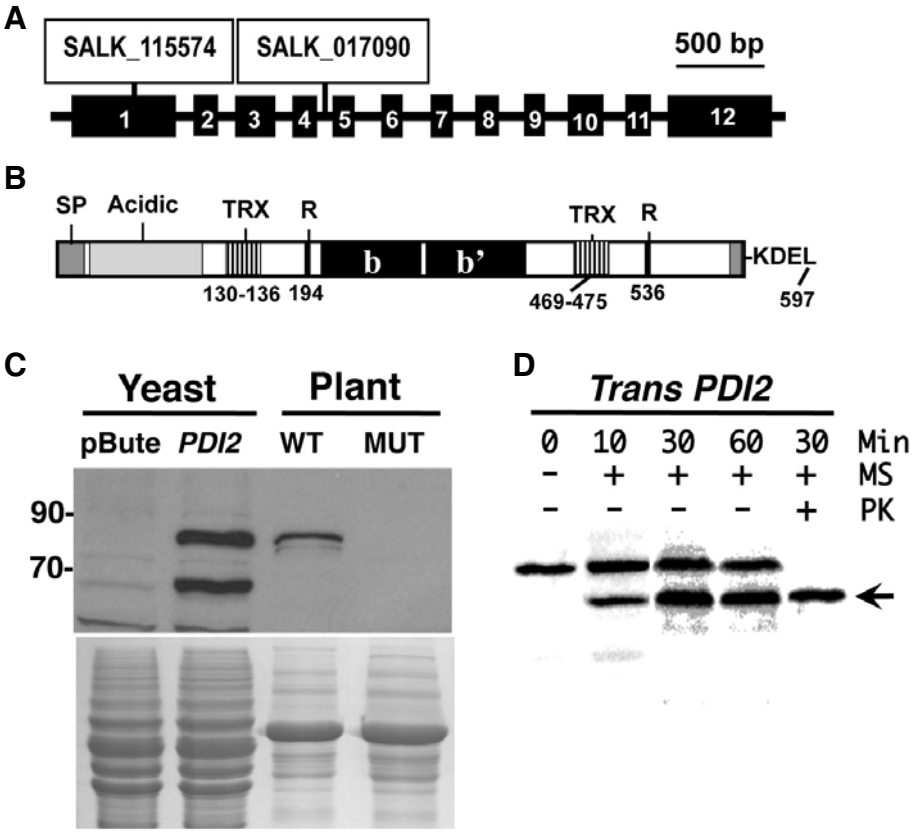

Fig. 1. *PDI2* gene and deduced protein organization, immunoblot analysis in wild type and the *pdi2* mutant, and microsomal processing of PDI2 *in vitro*. (A) *PDI2* gene locus (At5g 60640) organization. Exons are indicated by numbered black rectangles. The position of the T-DNA insertion is denoted by the boxed Salk mutant number in exon 1; bp, base-pair. (B) Predicted protein domain organization. SP, signal peptide (residues 1-25); acidic region; TRX, thioredoxin catalytic domain; b, b′ denote thioredoxin fold domains, R refers to a conserved catalytic arginine; ER-retention containing KDEL motif. The numbers under the polypeptide indicate positions of the amino acids in the protein sequence. (C) Immunoblot analysis using the PDI2-specific antiserum of the *PDI2* cDNA (lane PDI2) and empty vector (lane pBute) expressed in yeast and of total cellular proteins from wild type (WT) and *pdi2* T-DNA mutant (MUT) plants. Coomassie stained gels are shown under the blot to indicate uniform protein loading. Size standards are in kilodalton (kDa). (D) Microsomal processing of PDI2. The *Pdi2* cDNA was transcribed and translated *in vitro* with (+) and without (-) the presence of of canine microsomes (MS), for 10, 30 and 60 min (Min), followed by SDS-PAGE. The black arrowhead marks the processed product. Proteinase K (PK) was added to the 30 min reaction (+).

(ABRC, Ohio State University, USA) was used. To monitor fusion protein expression and localization, GFP was detected by excitation (laser power 30%) at 488 nm and using a 505-525 nm emission filter. The mCherry was detected by excitation at 543 nm (laser power 30%) and using a 560-620 nm emission filter. Photobleaching was performed by scanning nuclei with a 543 nm laser (laser power 90%) 20 times. FRET efficiency of the nucleus was calculated as the percentage change of the GFP intensity before and after bleaching with the equation of $E_{FRET} = (GFP_{after}-GFP_{before})/GFP_{after}X100$ (Bleckmann et al. 2010). We were able to fully separate GFP and mCherry spectra from chloroplast autofluorescence using the TCS SP5 microscope.

Electron microscopy and immunolabeling

For immunogold labeling analysis, developing roots and seeds were preserved by high-pressure freezing/freeze-substitution techniques as described (Ondzighi et al., 2008). Whole root tips and developing seeds were placed into an aluminum hat filled with 150 mM sucrose. The samples were frozen in a BALTEC HPM-010 High-Pressure Freezer (Technotrade, USA) and then transferred to liquid nitrogen for storage. Freeze-substitution was performed in 0.1% uranyl acetate plus 0.25% glutaraldehyde in anhydrous acetone in cryo-vials (Nunc, Denmark) for Lowicryl HM20 embedding for 7 days at -90°C, followed by slow warming to RT or -50°C, respectively, over a period of one day. After three rinses in acetone, samples were embedded in Lowicryl HM20 resin (EMS, USA): 33% (24 h), 66% (24 h), and 100% resin (3 days). Polymerization was carried out at -50°C under UV light for 2 to 3 days in flat bottom embedding capsules.

For immunolabeling, Lowicryl HM20 resin embedded sections were placed on formvar-coated gold or nickel slot grids and blocked for 30 min with 3% (w/v) non-fat dried milk solution in 0.01 M phosphate-buffered saline pH 7.2 containing 0.1% Tween-20 (PBST). The sections were washed and then incubated with a 10-fold dilution of the primary antibodies: anti-PDI2 or anti-GFP for 2 h at RT. Sections were washed and transferred to a 25-fold dilution of secondary antibody goat anti-rabbit IgG-conjugated to 10 or 15 nm gold particles (Ted Pella, Inc) for 2 h at RT. Sections were washed and then stained with uranyl acetate and lead citrate. All observations were performed using a Philips CM10 microscope (Philips, USA).

RESULTS

Protein disulfide isomerase-2, PDI2 (EC 5.3.4.1), is the largest of the 12 PDIs encoded in *Arabidopsis* genome (Lu and Christopher, 2008). The *PDI2* gene (accession No. At5g60640) contains 12 exons for a fully spliced sequence of 1794 bp, encoding a deduced polypeptide of 597 amino acids (BAB09837) (Fig. 1A). *PDI2* resides in a distinct phylogenetic subgroup of six members of the PDI family characterized by an *a-b-b′-a′* domain configuration (Lu and Christopher, 2008), similar to that of classical PDIs from *Homo sapiens* (HsPDI; 32% sequence identity to PDI2) and *Saccharomyces cerevisiae* (ScPDI1; 24% identity) (Supplementary Fig. 1). Among the members of this subgroup, PDI2 shares 56% sequence identity with PDI1 (At3g54960), and 29-32% identity with PDI3 (At1g52260), PDI4 (At3g16110), PDI5 (At1g21750) and PDI6 (At1g77510). Considerable variability exists within their active site (CXXC) se-

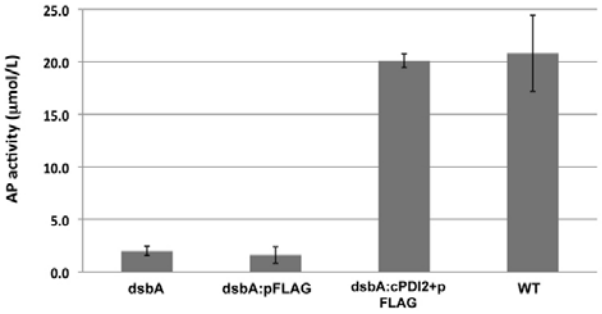

Fig. 2. Restoration of alkaline phosphatase activity by complementation of the *E. coli* protein folding mutant, *dsbA,* with the *Arabidopsis* PDI2 cDNA. The alkaline phosphatase activities (µmol/L · min) were measured in the dsbA mutant (R190) with (dsbA:pFLAG) and without (dsbA) the empty pFLAG expression vector, and with the PDI2 cDNA in the pFLAG expression vector (cPDI2+pFLAG), compared to the wild type *E. coli* (WT, strain R189). The data represent the average (± standard deviation) of three independent experiments with six replicates.

quences (Supplementary Fig. 2), suggesting that they may differ in their redox potential (Holst et al., 1997). All six of these PDIs are predicted to harbor both an N-terminal signal peptide and C-terminal ER retention signal KDEL (Lu and Christopher, 2008). Unlike classical PDIs, the *Arabidopsis* homologs do not possess an extended acidic C-terminal domain, although N-terminal regions of PDI1, PDI2, PDI3 and PDI4 are very rich in acidic Asp and Glu residues (Supplementary Fig. 2). The acidic regions of PDI1 and PDI2 are considerably longer than those found in PDI3 and PDI4. Two independent homozygous T-DNA insertions (SALK_115574 and SALK_017090) within exon-1 and intron-4, respectively, of the *PDI2* locus (Fig. 1A) were identified (Supplementary Fig. 3). The T-DNAs begin 523 bp and 1,330 bp, respectively, downstream from the initiator ATG codon of the predicted unspliced locus. Despite the absence of detectable PDI2 mRNA (Supplementary Fig. 3) and protein (Fig. 1C), no overt phenotype was discerned in the mutants. There was a slight decrease (10-12%) in germination rate of *pdi2* seeds relative to wild type.

A peptide unique to PDI2 was used to create a polyclonal peptide-specific PDI2 antiserum (described in the "Materials and Methods"). The antiserum was tested by immunoblot analysis of protein extracts from yeast cells expressing the *PDI2* cDNA, and of total cellular proteins from 14 day-old of *Arabidopsis* wild type and the *pdi2* T-DNA insertion mutant seedlings (Fig. 1C). The anti-PDI2 antiserum detected an ~75-80 KDa polypeptide in yeast and wild type *Arabidopsis*, which was slightly larger than the predicted MW of PDI2 (68 KDa). PDI2 protein was not detected in yeast cells containing the empty vector nor in the *Arabidopsis pdi2* T-DNA insertion mutant. The larger than expected band detected in both yeast and plants is likely due to N-glycosylation (three sites predicted) and the high level of acidic residues (117 D and E residues, 19.6%) (Supplementary Fig. 1), which can significantly retard the mobility of proteins separated by SDS-PAGE (Armstrong and Roman, 1993). The secondary band of 65 KDa in yeast was most likely a breakdown product that occurs in stationary phase cultures. This band was not observed in logarithmic phase cultures (Fig. 3B).

The SignalP software predicts a weak signal peptide to be cleaved between residues 25 and 26, which would remove a

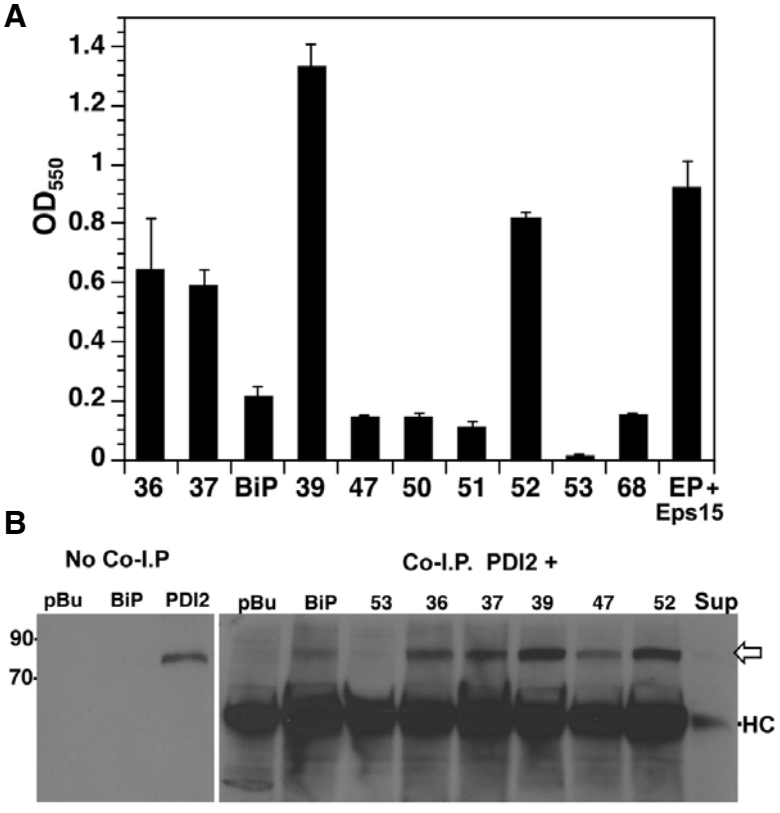

Fig. 3. Validation of protein interactions with the PDI2 bait obtained from the yeast two-hybrid assay (Table 2). (A) The β-galactosidase activity measurements were normalized to equal culture density of yeast cells co-expressing PDI2 bait plus each of the individual interacting proteins (designated by the number on the x-axis referred to in Table 2, ie Clone #39 is MEE8). Values of two negative controls (co-expression of interacting protein with empty bait vector; PDI2 bait expressed with empty prey vector) were subtracted from the plotted values. Means of two experiments in three replicates ± standard deviation are shown. The positive control (EP) consisted of Epsin 1 interacting with the EH domain-containing region of Eps15. No PDI2 was present in the EP/Eps15 cells (Rosenthal et al., 1999). (B) Immunoblot using the PDI2 antibody on co-immunoprecipitation (Co-I.P.) reactions. Each Co-I.P. contained PDI2 plus one of the HA-tag fused clones (numbered lanes from Table 2) and the anti-HA tag antiserum. The empty pBute vector (pBu) was the negative control. The supernatant of the Co-I.P reaction was included (Sup). Open arrowhead indicates co-immunoprecipitated PDI2 detected with the anti-PDI2 antiserum. The left three lanes were controls for no Co-I.P., in which 40 µg total yeast protein containing recombinant PDI2 or BiP or empty vector (pBu) was subjected to immunoblot analysis with the anti-PDI2 antiserum. The heavy chain (HC) of the anti-HA tag antiserum verified a uniform amount used in the Co-I.Ps.

Table 2. *Arabidopsis* proteins identified using the PDI2 bait in the yeast two-hybrid screen of *Arabidopsis* cDNA libraries.

Clone #	*Arabidopsis* locus, & accession #	Predicted protein	Predicted subcellular locales	Signal peptide	KDEL Seq.	cDNA library
36	At4g18740 NM_202840	Rho transcription termination family	Nucleus	No	No	seedling
37	At4g17730 AY074294	Syntaxin, SYP23	Tonoplast	No	No	seedling
38	At5g28540 NM_122737	Luminal binding protein, BiP1	Endoplasmic reticulum	Yes	HDEL	Seedling & stress
39	At1g25310 NM_102341	Maternal effect embryo arrest (MEE8), DNA binding- transcription factor, basic helix-loop-helix family	Nucleus, *KKKRR* 100% Nuclear localization signal	No	No	seedling
47	At2g21620 AY087097.1	Response to desiccation, RD2; Universal stress protein, ATP binding	Cytoplasm	No	No	stress
50	At5g09860 AF428323	Putative THO/TREX complex: HPR1	Nucleus	No	No	stress
51	At5g09660 AY057682	NAD-dependent malate dehydrogenase	Peroxisome	No	No	stress
52	At5g19590 BT002457	DUF538 domain protein	Secretory Path.	Yes	No	stress
53	At1g79930 NM_106642	Putative heat shock protein HSP91, HSP70	Nuclear (1) Cytoplasmic (2)	No	No	stress
68	At1g04410 AY065134	NAD-dependent malate dehydrogenase	Apoplast, Vacuole, Nucleus, Plastid	No	No	stress

~3 KDa peptide from PDI2. To test for the presence of a functional signal peptide, the PDI2 protein was assayed for processing by microsomal membranes (Bendtsen et al., 2004). The *PDI2* cDNA was transcribed and resulting mRNA translated in the presence of ^{35}S-MET *in vitro* with, and without, the addition of canine microsomal membranes. In the absence of microsomes, a single radiolabeled protein (upper band) is synthesized (Fig. 1D). When translation is conducted in the presence of microsomes for 10, 30 and 60 min, a processed product is detected (lower band, Fig. 1D). Treatment of the reaction after 30 min with proteinase-K resulted in degradation of the larger product, but the lower processed product resisted degradation, indicating uptake by microsomes. These results indicated that PDI2 contains a functional signal peptide that is cleaved, and the processed PDI2 protein is inserted into ER microsomes *in vitro*.

PDI2 restores alkaline phosphatase activity in the *E. coli* protein folding mutant, *dsbA*

A standard assay for protein folding activity of an enzyme is to test its capacity to complement the *dsbA* mutant of *E. coli*, which lacks protein-folding activity in the periplasm. Consequently, the *dsbA* mutation disrupts alkaline phosphatase activity, which is a homodimeric periplasmic enzyme that requires four intramolecular disulfides to function (Sone et al., 1997). The *omp*A periplasmic signal sequence was fused to the N-terminus of the full-length PDI2 cDNA in the pFLAG-CTS vector. This results in periplasmic secretion of the OMPA-PDI2 fusion protein. Expression of this construct in the *dsbA* mutant restored wild type levels of alkaline phosphatase activity, compared to the mutant alone and the mutant with the empty pFLAG vector (Fig. 2). This indicates that PDI2 complements the disulfide-based protein folding deficiency in the *dsbA* mutant.

Yeast two-hybrid screen identified putative PDI2-interacting proteins from the secretory pathway and nucleus

The significant expression of recombinant PDI2 in yeast (Fig. 1C) provided the opportunity to use the yeast two-hybrid assay to identify proteins that interacted with PDI2. Therefore, we screened two *Arabidopsis* cDNA libraries (seedling and stress-induced) for proteins interacting with PDI2 bait using the two-hybrid system. As shown in Table 2, the principal isolates were 10 clones that encoded the following proteins: ER-resident luminal binding protein involved in protein folding (Bip1); a maternal-effect embryo arrest factor (MEE8), which contains a strong nuclear localization signal and a basic-helix-loop-helix DNA binding motif; syntaxin; a desiccation-responsive RD2 protein; putative heat shock protein; transcription/RNA trafficking (HPR1); two NAD-dependent malate dehydrogenases, Rho-transcription termination-like protein; and one unknown protein (Table 2).

Two different validation tests were subsequently performed to verify the specificity of the interactions with PDI2. The first was β-galactosidase activities (β-gal) of the lacZ reporter gene (Fig. 3A), which were based on an equal cell culture density. This assay represents the degree of interaction between the positive candidates and PDI2 that productively activates *lacZ* gene expression. After subtracting the values obtained with the empty vector, MEE8 (clone #39) had the highest levels of β-gal activity, followed by protein 52 (DUF), and 36 (Rho Transcription termination-like protein), with syntaxin slightly lower in activity (Fig. 3A). Six candidates (e.g. BiP, RD2, GTP-binding protein, malate dehydrogenase) gave OD readings 0.2 or less.

The second validation test employed was the co-immuno-

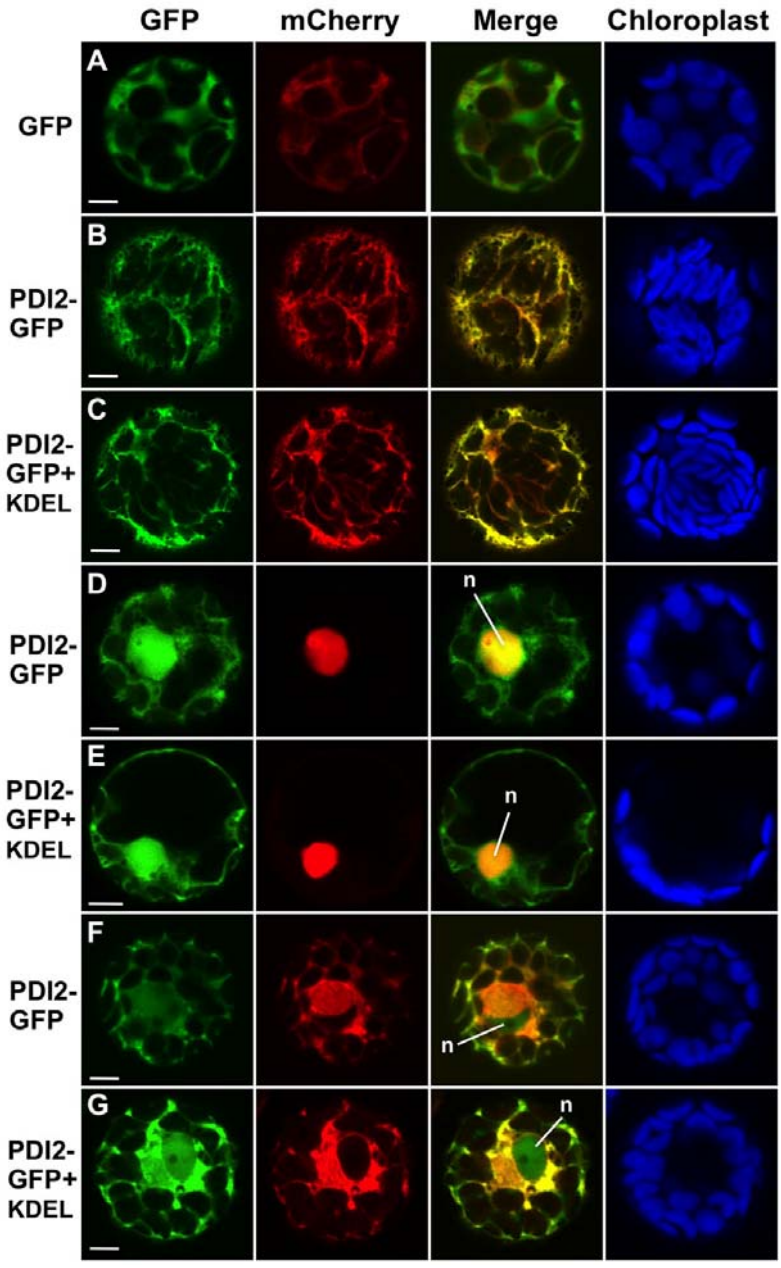

Fig. 4. Sub-cellular localization of PDI2-GFP and PDI2-GFP-KDEL co-expressed with three cellular markers fused to mCherry in mesophyll protoplasts as observed by laser scanning confocal microscopy. Emissions for GFP, mCherry, GFP + mCherry (merged) and chloroplasts are indicated at the top of the columns. (A) GFP co-expressed with the ER-mCherry marker; (B) PDI2-GFP co-expressed with the ER-mCherry marker; (C) PDI2-GFP-KDEL co-expressed with the ER-mCherry marker; (D) PDI2-GFP co-expressed with the MEE8-mCherry nuclear protein; (E) PDI2-GFP-KDEL co-expressed the MEE8-mCherry nuclear protein; (F) PDI2-GFP co-expressed with the gamma-TIP-mCherry vacuolar marker; (G) PDI2-GFP-KDEL co-expressed with the gamma-TIP-mCherry vacuolar marker. The n denotes nucleus. Scale bars represent 5 microns.

precipitation (co-IP) assay on seven representative positive clones (Fig. 3B). Each of the seven recombinant positive clones was fused to an HA-tag epitope, which is lacking in the recombinant PDI2. The anti-HA tag antiserum co-immunoprecipitated recombinant PDI2 only in the presence of the respective clone (Fig. 3B). The uniform efficiency of the initial precipitation with the Anti-HA antiserum is shown in Supplementary Fig. 4B. In general, the intensity of the band (Fig. 3B) correlated with the amount of β-gal activity (Fig. 3A), except for clone 36 (Rho), which had an OD over 0.6, but a relatively weaker band on the co-IP assay. Such differences in physical interaction (co-IP) relative to ß-gal activity could be due to steric hindrances, distal span of the protein that allows contact of the activation domain with the lacZ promoter, length of association-dissociation period and affinity for PDI2.

PDI2-GFP and PDI2-GFP-KDEL fusions localize to the ER, nucleus, and vacuole when transiently expressed in protoplasts

A subcellular targeting approach was next undertaken in live cells for two purposes. First, we sought to investigate the subcellular localizations of PDI2 using the *Arabidopsis* mesophyll protoplast transient expression system (Yoo et al., 2007). Second, we examined the localization of the PDI2 interactor, MEE8, which has a nuclear localization sequence. PDI2 fusions to the fluorescent reporter GFP(S65T) were developed with and without a C-terminal ER retrieval KDEL motif. Since the product encoded by *PDI2* contains a signal peptide at its N-terminus, GFP(S65T) was situated at the C-terminus of the PDI2-GFP fusion. To compensate for the burying of the KDEL motif in PDI2-GFP, a second fusion was developed in which the C-

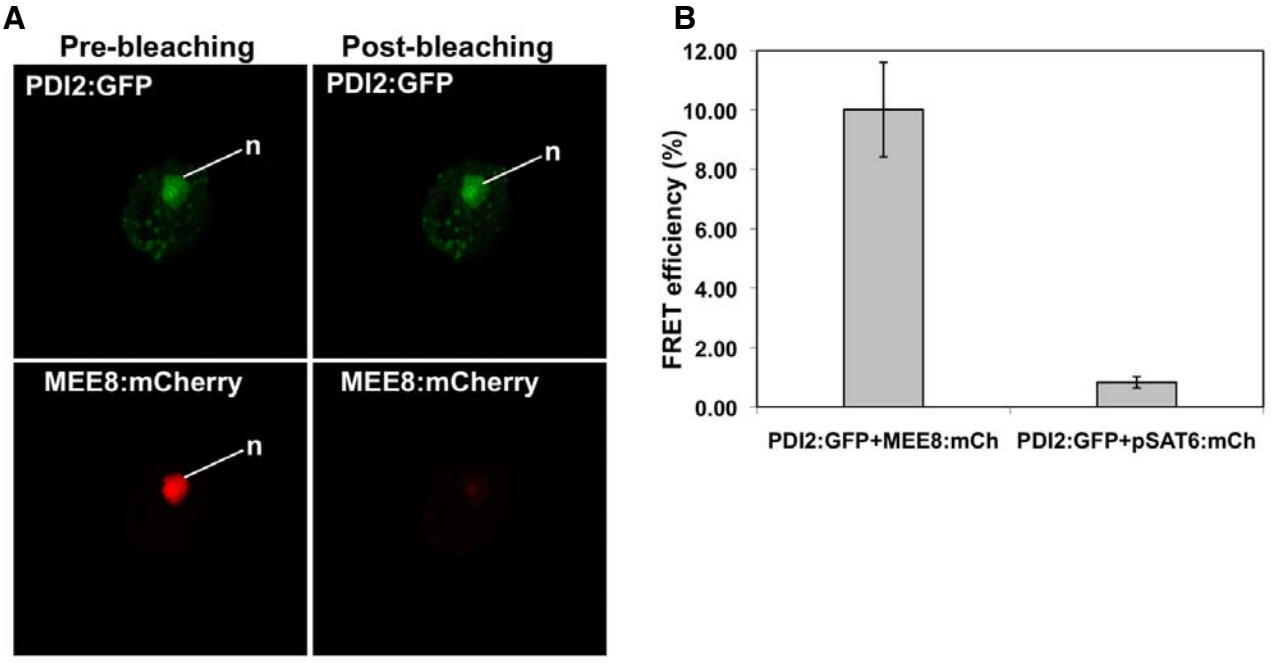

Fig. 5. Förster resonance energy transfer (FRET) between transiently expressed PDI2:GFP and MEE8:mCherry indicates protein-protein interaction between PDI2 and MEE8 in mesophyll protoplasts. (A) Confocal microscope images of the same protoplast exposed to 488 nm excitation (PDI2:GFP) or 543 nm excitation (MEE8:mCherry) before (pre-) and after (post-) bleaching the acceptor (mCherry) with 543 nm laser. The n denotes the nucleus. (B) The FRET efficiency was measured as the percent increase in GFP signal in the nucleus after bleaching the acceptor. The FRET efficiency was calculated for the PDI2:GFP and MEE8:mCherry pair and the PDI2:GFP and pSAT6:mCherry pair (pSAT6:mCh). The pSAT6 is a known nuclear protein that does not interact with PDI2, and thus serves as a negative control. The values represent FRET efficiencies calculated on 10 cells averaged ± SD. A FRET efficiency above 4% is considered to indicate close interaction between proteins for the GFP and mCherry pair (Bleckmann et al., 2010).

terminal end of GFP(S65T) was modified to include the KDEL motif, which we designated as PDI2-GFP-KDEL. Both fusions were analyzed concurrently via laser-scanning confocal microscopy (Fig. 4).

MEE8 and two secretory pathway markers (for the ER and vacuole) were fused to monomeric RFP variant, mCherry. They were co-expressed with PDI2-GFP fusions in leaf protoplasts (Fig. 4). The negative control, GFP alone, labeled the cytoplasm when co-expressed with the ER marker (Fig. 4A). The MEE8-mCherry labeled the nucleus (Figs. 4D and 4E). Both PDI-GFP and PDI-GFP-KDEL co-localized with the ER-marker-mCherry (Figs. 4B and 4C), the MEE8-mCherry (Figs. 4D and 4E), and the tonoplast marker (Figs. 4F and 4G). Approximately 20% of the protoplasts did not show GFP labeling in the nucleus, which we speculate could be related to cell development. PDI-GFP and PDI-GFP-KDEL were also observed in the nucleus when co-expressed with the vacuolar marker, depending on the section of the cell imaged (Figs. 4F and 4G). However, to observe the GFP label in the vacuole, the constructs had to be incubated in protoplasts for longer periods after transfection (i.e. 20-24 h). Regardless, the presence of the C-terminal KDEL on the fusion protein did not cause the protein to be retained in the ER. Therefore, the co-expression of subcellular markers with PDI2-GFP constructs in live protoplasts indicated dual secretory and non-secretory localizations of PDI2. The dual localizations were not due to aberrant post-translational cleavage of the PDI2 from the GFP, as determined by immunoblot analysis of the intact PDI2-GFP fusion expressed in protoplasts (Supplementary Fig. 4).

Interaction of PDI2 with MEE8 *in vivo* as measured by FRET

Because PDI2 and the nuclear MEE8 were determined to interact in the yeast two-hybrid assay and via co-immunoprecipitation *in vitro* (Fig. 3), it would be critical to test if they interacted in plant cells *in vivo*. The co-localization of the PDI2-GFP and MEE8-mCherry fusion proteins to the nucleus (Fig. 4) provided the means to test this interaction *via* Förster resonance energy transfer (FRET). The GFP emission spectrum partially overlaps with the mCherry excitation spectrum. For energy to be transferred from GFP to mCherry, then the two proteins must be very close (< 10 nm) and oriented properly. The PDI2-GFP and MEE8-mCherry constructs were co-expressed in mesophyll protoplasts and were analyzed by confocal laser scanning microscopy (Fig. 5A). As a negative control, the PDI2-GFP and SAT6-mCherry were co-expressed and analyzed in parallel. The SAT6 is a known nuclear protein that is not expected to interact with PDI2 and produce FRET (Zaltsman et al., 2007). We measured FRET efficiency using the acceptor photobleaching method in which donor GFP fluorescence is quantified before and after photobleaching of the acceptor mCherry. FRET efficiency was calculated with changes in the GFP intensity from nuclei after bleaching mCherry (Fig. 5A). The ~10% increase in donor (PDI2-GFP) intensity simultaneously with a decrease in the acceptor (MEE8-mCherry) fluorescence after bleaching indicated energy transfer relative to the negative control pair (Fig. 5B). A FRET efficiency above 4% is considered to indicate close interaction between proteins for the GFP and mCherry pair (Bleckmann et al., 2010). Therefore,

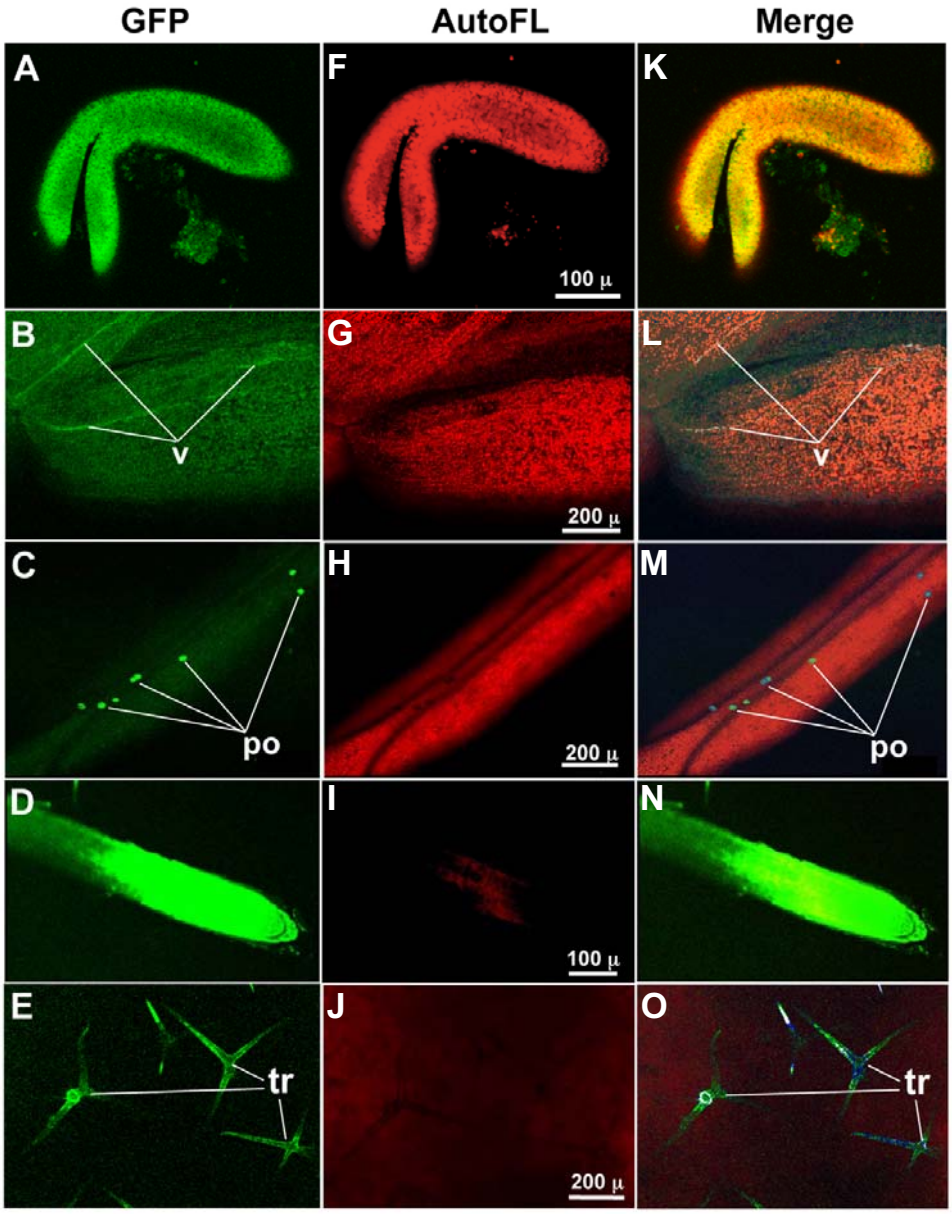

Fig. 6. Analysis of the expression of the native *PDI2*-promoter-N-terminus-GFP fusion expressed in *Arabidopsis* seedlings (A, B, and C), leaves and leaf vascular tissue (v) (D, E, and F), stamen and pollen (po, G, H, and I), root tips (J, K, and L) and leaf trichomes (tr, M, N, and O). The left column shows the GFP-specific filter on the confocal microscope. The center column has the red chlorophyll autofluorescence (AutoFl). The right column is the combined images of GFP and chlorophyll autofluorescence (merge). Bar indicates size in microns (µ).

FRET efficiency results indicated that PDI2 and MEE8 interacted *in vivo*.

PDI2 is expressed in a variety of plant tissues with enhanced levels in root tips and developing seeds

As a prerequisite for a high-resolution sub-cellular analysis of PDI2 localization, the expression of *PDI2* was examined in various tissues in the plant. A native *PDI2* gene promoter-PDI2-GFP4 fusion was expressed in stable transgenic plants. This construct was predicted to reproduce virtually native expression levels in the plant and was also subsequently used with TEM for subcellular localization (Fig. 8). Four independent transgenic lines were assessed and the representative results are indicated (Figs. 6 and 7). Robust PDI2-GFP expression was observed microscopically throughout the 2 day-old germinating seedling, including the cotyledons and hypocotyl (Fig. 6A). Weaker expression was observed in leaves (underside) with enhanced levels in vascular regions from 21 day-old plants (Fig. 6B). Interestingly, high levels of GFP expression occurred in pollen grains on the surface of the stamens (Fig. 6C), in root tips (Fig. 6D) and leaf trichomes (Fig. 6E). Developing seeds and siliques were prominently labeled with GFP (Fig. 7), especially the perimeter cell layers of the developing seed at ~14 and 18 days post-fertilization (Figs. 7A and 7B). Scanning the surface layer of the seed (Fig. 7C), GFP levels were particularly high in the outer cells, intercellular spaces (cell wall, plasma

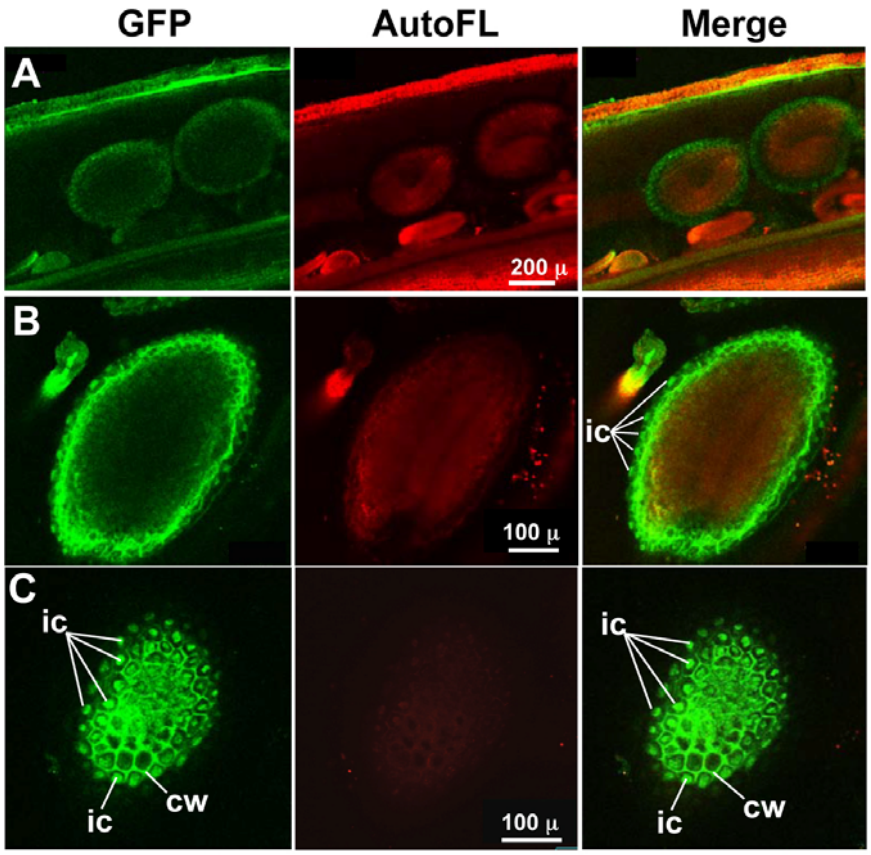

Fig. 7. Analysis of the expression of the native *PDI2*-promoter-N-terminus-GFP fusion expressed in developing siliques (A) and seeds (A, B, and C) of *Arabidopsis* and the impact of the *pdi2* mutant on the seed phenotype. In (C), a different scanning plane of the top seed surface was imaged on the confocal microscope that revealed GFP label in the cell wall (cw) inner cellular structures (ic). The center column presents the red chlorophyll autofluorescence (AutoFl). The right column combines the images of GFP and chlorophyll autofluorescence (merge). Bar indicates size in microns (μ).

membrane, apoplasm) and within large internal cellular structures. These observations of *PDI2* gene expression in various tissues coincide with observations compiled at the microarray level (Supplementary Fig. 5).

PDI2-GFP and PDI2 localize to the ER, Golgi, vacuole, apoplasm and nucleus

To precisely characterize the subcellular localization of PDI2, immunogold electron microscopy was performed on ultra-thin sections of high-pressure frozen, acetone-substituted tissues. In one set of experiments, anti-GFP antibodies were used to detect the PDI2-GFP reporter fusion in developing seeds from PDI2-Pr-Nter-GFP4 transgenic plants (Fig. 8). In a second set of experiments, the anti-PDI2 antiserum was used on wild-type root samples (Figs. 8 and 9). These tissues were selected for analysis due to their relatively high level of *PDI2* gene expression and amenability to cryofixation. In this way, two different antibodies on two distinct tissues (transgenic seed vs. wild type root) serve as complementary controls to verify labeling of similar subcellular structures.

In transgenic *PDI2*-Pr-Nter-GFP4 developing seeds, the anti-GFP antiserum labeled the ER (Figs. 8A and 8C), Golgi and Golgi-associated vesicles (Fig. 8B), vacuolar contents (Fig. 8C), cell wall, plasma membrane-cell wall (Fig. 8D) and the nucleus and nuclear membrane (Fig. 8E). No label was observed with the GFP antiserum on sections of wild type plants (Supplementary Fig. 6). When ultra-thin sections of wild type root tissues were labeled with the PDI2 antiserum followed by anti-rabbit 15 nm gold secondary antiserum (Fig. 9), the labeling was detected in the ER (Fig. 9A), Golgi apparatus and associated vesicles (Fig. 9B), the cell wall (Fig. 9C), cell wall and plasma membrane (Fig. 9D), and vacuolar contents (Fig. 9E and Fig. 9F). The nucleus was also labeled (Fig. 10), the nucleoplasm (Figs. 10B and 10C) as well as the nuclear pore, nuclear membrane and surrounding cytoplasm (Fig. 10C). No label was detected with pre-immune serum and secondary antibody controls in wild type roots (Supplementary Fig. 7). In summary, using two different antisera (the anti-GFP and anti-PDI2) on two distinct types of tissues (transgenic seed and wild type roots, respectively), similar organelles and subcellular structures were labeled including various segments of the secretory pathway and the nucleus. These localizations corresponded to the in vivo targeting of reporters in protoplasts (Fig. 4) and predicted sub-cellular locations of the interacting proteins identified in the yeast-two-hybrid screen (Table 2).

DISCUSSION

PDI2 stimulates protein folding, localizes to the ER and interacts with an ER protein folding chaperone

PDI and PDI-like proteins have been implicated in a wide range of processes in animals, but our understanding of PDIs in plants has been limited. In particular, we know very little about the activities of plant PDIs, where they are located in the cell and the proteins that interact with them. Here we describe a functional role in protein folding and have identified novel secretory and non-secretory subcellular localizations and protein-protein interactions for a new PDI2 from *Arabidopsis*. PDI2 complemented the *E. coli dsbA* mutant, which is defective in the disulfide-based folding of secreted polypeptides in the perip-

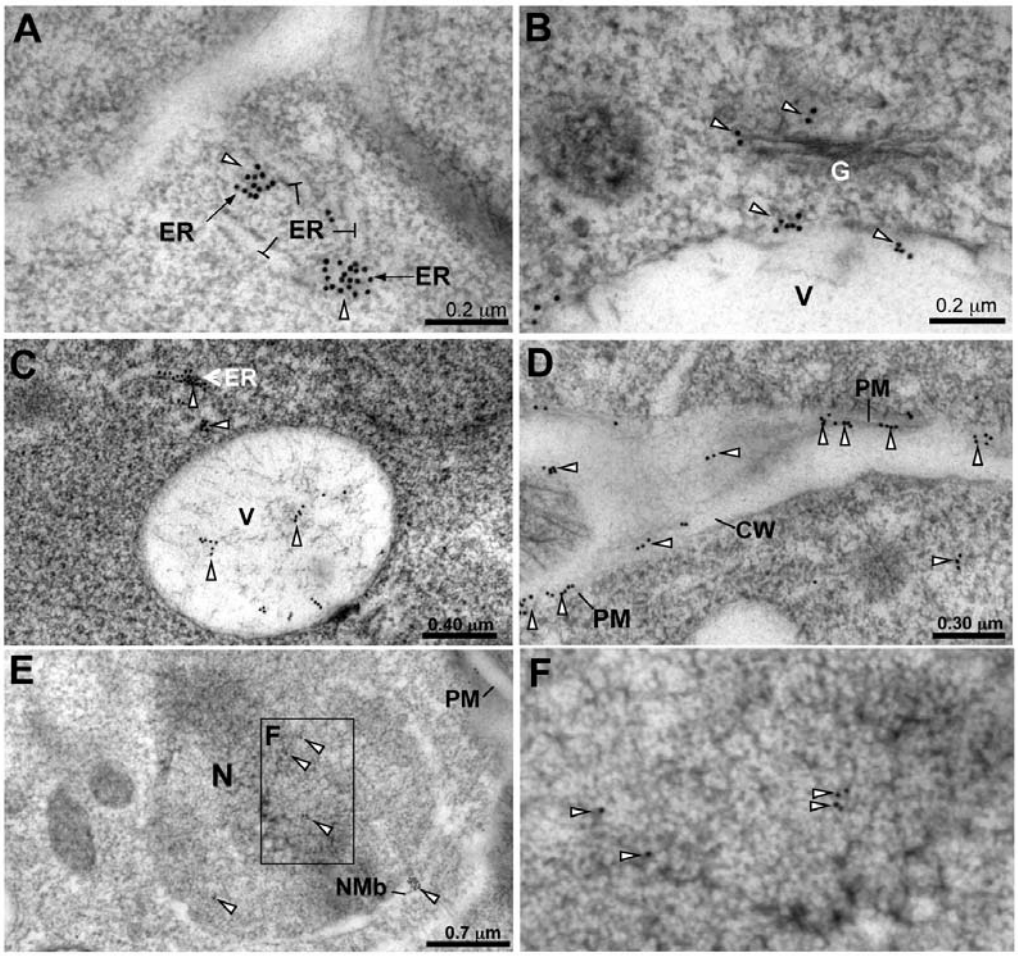

Fig. 8. TEM analysis after immunolabeling of seed sections from transgenic *Arabidopsis* expressing the native *PDI2*-promoter-N-terminus-GFP fusion as shown in Fig. 7. The GFP-specific antiserum followed by gold conjugated secondary antiserum were used. Immuno-gold labeling of GFP was observed in (A), endoplasmic reticulum (ER); (B), Golgi (G), and vacuole (V); (C), ER and vacuole; (D), apoplasm and plasma membrane (PM) and cell wall (CW); (E), nucleus (N) and nuclear membrane (NMb), (F), enlargement of nuclear subregion in (E).

lasm (Ostermeier et al., 1996), leading to a lack of alkaline phosphatase activity. Alkaline phosphatase is a homodimeric periplasmic enzyme that requires two intramolecular disulfides in each subunit for proper folding and activity (Sone et al., 1997). PDI2 significantly reconstituted alkaline phosphatase activity in this mutant, indicating that the enzyme was properly folded. The protein folding activity of PDI2 is consistent with its primary structure and thioredoxin domain organization, which are conserved with human and mammalian PDIs, involved in classical ER-based protein folding. The uptake of PDI2 into microsomes *in vitro* (Fig. 1), its localization to the ER *in vivo* (Figs. 4, 8, 9 and 10) and its interaction (Table 2, Fig. 3) with the ER luminal protein-folding chaperone and binding protein, BiP (Bertolotti et al., 2000; Xu et al., 2005), further indicated a role of PDI2 in protein folding.

Mammalian PDI and BiP act synergistically *in vitro* in the oxidative folding of denatured and reduced Fab fragments (Mayer et al., 2000), and comprise a complex that includes both calcium binding protein 1 (CABP1) and the PDI-like ER protein (ERp72), termed the translocon-resident-PDI (TR-PDI) complex (Stockton et al., 2003). The ability of PDI2 and BiP to interact in yeast and *in vitro* raises the possibility that the two enzymes may cooperate to facilitate protein folding as part of a heteromeric complex in *Arabidopsis*. Our yeast two-hybrid screen also identified two members of the malate dehydrogenase (MDH) family as potential interactors of PDI2 (Table 2, At1g04410 and At5g09660). We speculate that these are potential substrates for PDI2, as experiments performed in vitro have demonstrated that porcine PDI can bind partially folded mitochondrial MDH (K_d = 0.2 μm) and facilitate its refolding (Cheung and Churchich, 1999). Two other PDI2-interactors were the response to desiccation protein, RD2 (Kerk et al., 2003), and with syntaxin, which functions in exocytosis of secreted proteins (Battey et al., 1999). Further experiments will be necessary to establish the exact biochemical mechanisms of the protein interactions and if the molecular associations occur *in planta*.

PDI2 interacts with transcription factor, MEE8, in the nucleus *in vivo*

Interestingly, the strongest interacting protein isolated from our yeast two-hybrid screen and *in vitro* co-IP assays corresponded to MEE8, a basic helix-loop-helix (bHLH) class transcription factor. The interaction with PDI2 with MEE8 in the nucleus *in vivo* was confirmed by FRET in plant protoplasts. This suggested that PDI2 acts upon MEE8 or functions in a complex with it. There is precedent for the involvement of PDIs in the

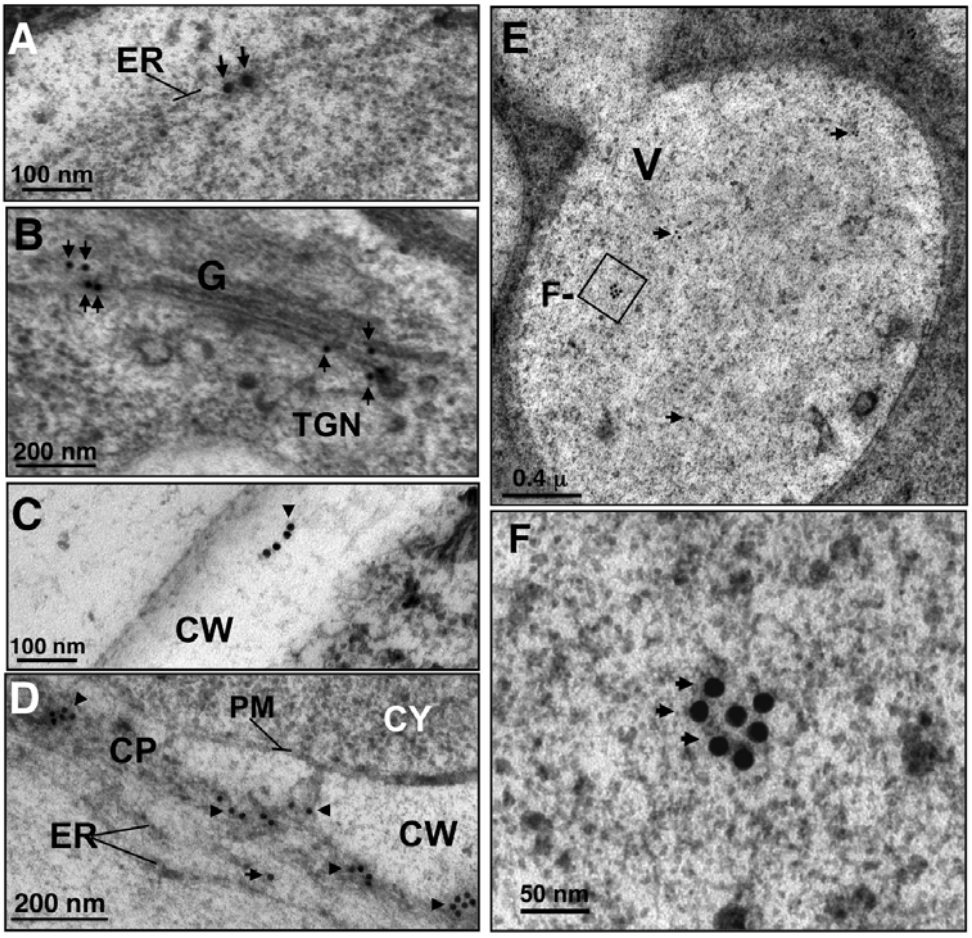

Fig. 9. TEM analysis after immunolabeling of wild type *Arabidopsis* root sections with the PDI2-specific antiserum and 15 nm gold secondary antiserum (arrowheads). (A) PDI2 labeling detected in the endoplasmic reticulum (ER); (B) Golgi apparatus (G) and trans-Golgi region (TGN); (C) cell wall-apoplasm (CW); (D) newly forming cell plates (CP) and plasma membrane (PM), cytoplasm (CY); (E, E1) vacuole (V). (E1) is an enlargement of labeling within the vacuole delimited by the smaller rectangle within (E).

regulation of transcription factor activity. HsPDI, and the PDI-like glucose-regulated protein 58 (ERp57/GRP58), are capable of regulating the formation of an intermolecular disulfide cross-link between monomers of the bHLH transcription factor E2A (Markus and Benzera, 1999). This disulfide crosslink is required for the stable binding of homodimeric E2A to DNA. HsPDI may also regulate the activity of the transcription factor NF-κB (Clive and Greene, 1996; Higuchi et al., 2004). The strong expression of PDI2 in the outer cell layers of the seed, and its localization to the nucleus in these cells, are intriguing when the interaction of PDI2 with MEE8 is considered. MEE8 is believed to play a role in regulating genes in maternal tissue necessary for normal embryo and endosperm biogenesis (Pagnussat et al., 2005). MEE8 possesses four cysteine residues, which could be involved in PDI2-mediated disulfide bond formation, with residue C96 being a strong candidate for further analysis due to its conservation among several *Arabidopsis* bHLH proteins. In addition to MEE8, our yeast two-hybrid screen identified two other nuclear interactors of PDI2: HPR1 (At5g09860), a component of the THO/TREX mRNA export complex (Furumizu et al., 2010; Jauvion et al., 2010); and a protein sharing partial homology to the prokaryotic Rho transcription termination factor.

PDI2 exited the ER and trafficked through the secretory pathway

PDI2 was demonstrated to have a functional 25-residue signal peptide that is co-translationally processed *in vitro* and inserted into canine microsomal membranes. The signal peptide is necessary for co-translational insertion through the ER membrane into the lumen (Bendtsen et al., 2004), where the KDEL sequences assist ER retention. In wild type and transgenic plants and leaf mesophyll protoplasts, PDI2 localized to the ER and also departed the ER, despite the presence of a KDEL sequence, and trafficked to various compartments of the secretory pathway (vacuole, Golgi, plasma membrane and cell wall). Similarly, other KDEL-containing proteins in plants traffic from the ER to different subcellular destinations. We recently showed that PDI5-KDEL is a chaperone of cysteine proteases, which are transported together from the ER to the Golgi and protein storage vacuoles (Ondzighi et al., 2008). In castor bean, KDEL-tailed cysteine proteases leave the ER and enter vacuoles (Helm et al., 2008). An auxin-binding protein with a KDEL sequence exits the ER and travels to the plasma membrane (Jones and Herman, 1993). Likewise, in rat exocrine pancreatic cells, a PDI containing a KDEL signal traffics from the ER

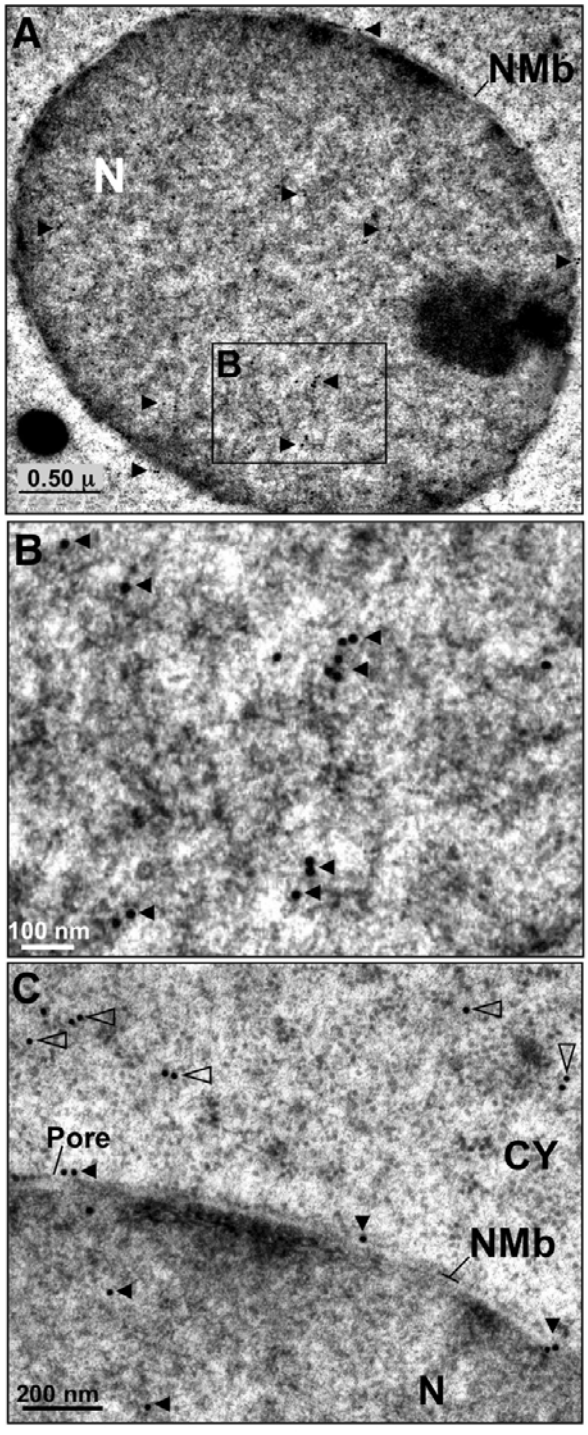

Fig. 10. TEM analysis of nucleus after immunolabeling of wild type *Arabidopsis* root sections with the PDI2-specific antiserum and 15 nm gold secondary antiserum (arrowheads). (A) PDI2 labeling detected in the entire nucleus (N) and nuclear membrane (NMb). (B) Enlargement of nuclear matrix from (A) showing discrete labeling; (C) Enlargement of nucleus, nuclear membrane (NMb) and cytoplasm (CY) indicating labeling in these regions and in a nuclear pore. Labeling in the cytoplasm is differentiated with white arrowheads.

through the secretory pathway to the plasma membrane (Turano et al., 2002; Yoshimori et al., 1990). The KDEL motif at the C-terminus of PDI2 may ensure temporary ER residency, but could be overridden by other signals to allow export from the ER to the Golgi, vacuole or apoplasm. The interaction with a substrate protein might obscure or inactivate the PDI2-KDEL signal, thus allowing transport out of the ER. Of the proteins that interacted with PDI2 (Table 2), only the ER protein folding chaperone, BiP, contained an ER-retention motif. In some cases, PDI and BiP of the vacuole reportedly lack their C-terminal ER retention signals (Tamura et al., 2004). In contrast to our results, the PDI observed in the vacuole was not found in the Golgi (Tamura et al., 2004). This discrepancy may be due to the glycosylation of PDI2 in the Golgi and/or the need to transport PDI2 to the cell wall.

Mechanisms for dual localization of PDI2 to the nucleus and secretory pathway

Intriguingly, PDI2 also trafficked from the cytosol to a non-secretory compartment, the nucleus (Figs. 4, 8, 9, and 10). Thus, this work raises the significant question about how PDI2 can enter both the secretory and non-secretory pathways. Mammalian PDI is cellularly distributed beyond the ER, with reports of its detection in the cytosol, cell surface and the nucleus (reviewed in Turano et al., 2002). Examples of proteins that exhibit dual localization to the ER and nucleus include the PDI homolog ERp57/GRP58 (Adikesavan et al., 2008), yeast ubiquitin ligase (Swanson et al., 2001), and parathyroid related protein (Amaya et al., 2008). However, in each of these examples, the corresponding precursor polypeptide contains both a signal peptide and a nuclear localization signal (NLS). PDI2 is not predicted to harbor a NLS, although ~43% of the known nuclear proteins in yeast also do not possess an obvious NLS (Lange et al., 2007), and several nuclear proteins lacking a NLS have been described in plants (Kong et al., 2006; Pomeranz et al., 2009) and animals (Asally and Yoneda, 2005; Rout et al., 2003). Thus, it is possible that PDI2 contains a new type of NLS, or is directed into the nucleus through an NLS-independent mechanism as has been hypothesized for other nuclear proteins (Kong et al., 2006; Pomeranz et al., 2009).

A different mechanism for dual localization of PDI2 invokes the nascent polypeptide-associated complex (NAC) (Powers and Walter, 1996), which modulates interactions that occur between the ribosome-nascent polypeptide chain complex, the signal recognition particle (SRP) and the ER membrane (Favaloro et al., 2008; Jackson and Blobel 1977). Accordingly, NAC would compete with SRP for the nascent PDI2. NAC binding diverts the PDI2 to a non-secretory pathway (i.e. the nucleus), whereas SRP binding would lead to co-translational insertion into the ER. This mechanism has been proposed for the dual localization of the PDI, RB60 (which contains a signal peptide and C-terminal KDEL), to the ER and chloroplast in *Chlamydomonas* (Levitan et al., 2005). Post-translational insertion of the signal peptide-containing polypeptide was observed in a few cases in animals, yeast and plants (Cramer et al., 1987; Plath et al., 1998; Rapoport et al., 1999). Alternatively, PDI2 could enter the nucleus by interacting with MEE8, which has a strong NLS (Table 2) that can mask the signal peptide (Karniely and Pines, 2005).

The lack of a *pdi2* mutant phenotype suggests functional redundancy

Despite the broad gene expression pattern of *PDI2*, the two independent *pdi2-1* and *pdi2-2* T-DNA insertion mutants do not display an obvious mutant phenotype under normal laboratory

growth conditions, and do not exhibit altered sensitivity to DTT, a known inducer of UPR (Yuen, Cho and Christopher, unpublished data). The high level of *PDI2* expression in embryos, the endosperm, and especially the seed coat (Fig. 7; Supplementary Fig. 5) suggested that its gene product may play a role in female gametophyte, embryo, or seed development. Indeed, two of the PDI2 interactors identified in our yeast two-hybrid screen, BiP1 and MEE8, have been implicated in these processes. *BiP1* and its homolog *BiP2* are functionally redundant, and female gametophyte defective at both loci are unable to undergo polar nuclei fusion following pollen fertilization (Maruyama et al., 2010). A *Ds* insertion within *MEE8* was identified in a genetic screen for mutants altered in female gametophyte development, and displayed abnormal endosperm development and embryo arrest at the one-cell zygotic stage (Pagnussat et al., 2005). We do not observe similar defects associated with either *pdi2-1* or *pdi2-2*, and Ruthenium red staining indicated that mutant seeds were able to produce mucilage upon hydration (Cho, Yuen and Christopher, unpublished data). Given the overlapping expression patterns of multiple *a-b-b′-a′* type PDI genes across *Arabidopsis* tissues (Supplementary Fig. 5), and the ability of two members (*PDI1* and *PDI5*) to be upregulated by UPR (Lu and Christopher, 2008), we hypothesize that functional redundancy may compensate for the loss of *PDI2*. Thus, the generation of plants defective at one or more additional *PDI* genes will be necessary to observe a phenotype associated with *pdi2*.

In conclusion, the *Arabidopsis* PDI homolog, PDI2, is an ER resident protein involved in protein folding and interacts with the protein-folding chaperone, Bip. PDI2 is also found in several non-ER locations, most notably the nucleus. Our findings support the idea that PDIs have functional roles that extend beyond the ER lumen. The identification of MEE8, which interacted with PDI2 in the nucleus in plants *in vivo*, provided an important clue for further research into a novel function of PDI2 associated with MEE8 and mechanisms for dual protein localization.

Note: Supplementary information is available on the Molecules and Cells website (www.molcells.org).

ACKNOWLEDGMENTS

We thank Dr. Dong-Ping Lu for assistance with the transcription-translation experiments. This work was supported by the National Science Foundation (grant No. MCB-09-58107) awarded to DAC and BHK.

REFERENCES

Adikesavan, A., Karani, U., Emmanual, J., and Anil, K. (2008). Overlapping signal sequences control nuclear localization and endoplasmic reticulum retention of GRP58. Biochem. Biophys. Res. Commun. *377*, 407-412.

Amaya, Y., Nakai, T., Komaru, K., Tsuneki, M., and Miura, S. (2008). Cleavage of the ER-targeting signal sequence of parathyroid hormone-related protein is cell-type-specific and regulated in cis by its nuclear localization signal. J. Biochem. *143*, 569-579.

Armstrong, D.J., and Roman, A. (1993). The anomalous electrophoretic behavior of the human papillomavirus type 16 E7 protein is due to the high content of acidic amino acid residues. Biochem. Biophys. Res. Commun. *192*, 1380-1387.

Asally, M., and Yoneda, Y. (2005). Beta-catenin can act as a nuclear import receptor for its partner transcription factor, lymphocyte enhancer factor-1 (lef-1). Exp. Cell. Res. *308*, 357-363.

Aslund, F., and Beckwith, J. (1999). Bridge over troubled waters: sensing stress by disulfide bond formation. Cell *96*, 751-753.

Battey, N.H., James, N.C., Greenland, A.J., and Brownlee, C. (1999). Exocytosis and Endocytosis. Plant Cell *11*, 643-659.

Bendtsen, J.D., Nielsen, H., von Heijne, G., and Brunak, S. (2004). Improved prediction of signal peptides: SignalP 30. J. Mol. Biol. *340*, 783-795.

Bertolotti, A., Zhang, Y., Hendershot, L.M., Harding, H.P., and Ron, D. (2000). Dynamic interaction of BiP and ER stress transducers in the unfolded-protein response. Nat. Cell. Biol. *2*, 326-332.

Bleckmann, A., Weidtkamp-Peters, S., Seidel, C.A., and Simon, R. (2010). Stem cell signaling in *Arabidopsis* requires CRN to localize CLV2 to the plasma membrane. Plant Physiol. *152*, 166-176.

Cheug, P.Y., and Churchich, J.E. (1999). Recognition of protein substrates by protein-disulfide isomerase A sequence of the b′ domain responds to substrate binding. J. Biol. Chem. *274*, 32757-61.

Christopher, D.A., Borsics, T., Yuen, C.Y., Ullmer, W., Andème-Ondzighi, C., Andres, M.A., Kang, B.H., and Staehelin, L.A. (2007). The cyclic nucleotide gated cation channel AtCNGC10 traffics from the ER *via* Golgi vesicles to the plasma membrane of *Arabidopsis* root and leaf cells. BMC Plant Biol. *7*, 1471-2229.

Chun, L., Kawakami, A., and Christopher, D.A. (2001). Phytochrome A mediates blue light and UV-A dependent chloroplast gene transcription in green leaves. Plant Physiol. *125*, 1957-1966.

Clive, D.R., and Greene, J.J. (1996). Cooperation of protein disulfide isomerase and redox environment in the regulation of NF-κB and AP1 binding to DNA. Cell Biochem. Funct. *14*, 49–55.

Clough, S., and Bent, A. (1998). Floral dip: a simplified method for *Agrobacterium*-mediated transformation of *Arabidopsis thaliana*. Plant J. *16*, 735-743.

Cokol, M., Nair, R., and Rost, B. (2000). Finding nuclear localisation signals. EMBO Rep. *1*, 411-415.

Couet, J., De Bernard, S., Loosfelt, H., Saunier, B., Milgrom, E., and Misrahi, M. (1996). Cell surface protein disulfide-isomerase is involved in the shedding of human thyrotropin receptor ectodomain. Biochemistry *35*, 14800-14805.

Cramer, J.H., Lea, K., Schaber, M.D., and Kramer, R.A. (1987). Signal peptide specificity in post-translational processing of the plant protein phaseolin in *Saccharomyces cerevisiae*. Mol. Cell. Biol. *7*, 121-128.

Durfee, T., Becherer, K., Chen, P.L., Yeh, S.H., Yang, Y., Kilburn, A.E., Lee, W.H., and Elledge, S.J. (1993). The retinoblastoma protein associates with the protein phosphatase type 1 catalytic subunit. Genes Dev. *7*, 555-569.

Favaloro, V., Spasic, M., Schwappach, B., and Dobberstein, B. (2008). Distinct targeting pathways for the membrane insertion of tail-anchored (TA). proteins. J. Cell Sci. *121*, 1832-1840.

Ferrari, D.M., and Soling, H.D. (1999). The protein disulphide-isomerase family: unraveling a string of folds. Biochem. J. *339*, 1-10.

Fields, S., and Song, O. (1989). A novel genetic system to detect protein-protein interactions. Nature *20*, 245-246.

Finn, R.D., Mistry, J., Schuster-Böckler, B., Griffiths-Jones, S., Hollich, V., Lassmann, T., Moxou, S., Marshall, M., Khanna, A., Durbin, R., et al. (2006). Pfam: clans, web tools and services. Nucleic Acids Res. *34*, D247-D251.

Frand, A.R., and Kaiser, C.A. (1998). The ERO1 gene of yeast is required for oxidation of protein dithiols in the endoplasmic reticulum. Mol. Cell *1*, 161-170.

Furumizu, C., Tsukaya, H., and Komeda, Y. (2010). Characterization of EMU, the *Arabidopsis* homolog of the yeast THO complex member HPR1. RNA *16*, 1809-1817.

Gruber, C.W., Cemazar, M., Heras, B., Martin, J.L., and Craik, D.J. (2006). Protein disulfide isomerase: the structure of oxidative folding. Trends Biochem. Sci. *31*, 455-464.

Gruber, C.W., Cemazar, M., Clark, R.J.T., Renda, R.F., Anderson, M.A., and Craik, D.J. (2007). A novel plant protein-disulfide isomerase involved in the oxidative folding of cystine knot defense proteins. J. Biol. Chem. *282*, 20435-20446.

Haseloff, J., Siemering, K.R., Prasher, D.C., and Hodge, S. (1997). Removal of a cryptic intron and subcellular localization of green fluorescent protein are required to mark transgenic *Arabidopsis* plants brightly. Proc. Natl. Acad. Sci. USA *94*, 2122-2127.

Helm, M., Schmid, M., Hierl, G., Terneus, K., Tan, L., Lottspeich, F., Kieliszewski, M.J., and Gietl, C. (2008). KDEL-tailed cysteine endopeptidases involved in programmed cell death, intercalation of new cells, and dismantling of extensin scaffolds. Am. J. Bot. *95*, 1049-1062.

Higuchi, T., Watanabe, Y., and Waga, I. (2004). Protein disulfide isomerase suppresses the transcriptional activity of NF-κB. Bio-

chem. Biophys. Res. Commun. *318*, 46-52.
Holst, B., Tachibana, C., and Winther, J.R. (1997). Active site mutations in yeast protein disulfide isomerase cause dithiothreitol densitivity and a reduced rate of protein folding in the endoplasmic reticulum. J. Cell. Biol. *138*, 1229-1238.
Honscha, W., Ottallah, M., Kistner, A., Platte, H., and Petzinger, E. (1993). A membrane-bound form of protein disulfide isomerase (PDI). and the hepatic uptake of organic anions. Biochim. Biophys. Acta *1153*, 175-183.
Houston, N.L., Fan, C., Xiang, J.Q., Schulze, J.M., Jung, R., and Boston, R.S. (2005). Phylogenetic analyses identify 10 classes of the protein disulfide isomerase family in plants, including single-domain protein disulfide isomerase-related proteins. Plant Physiol. *137*, 762-778.
Jackson, R.C., and Blobel, G. (1977). Post-translational cleavage of presecretory proteins with an extract of rough microsomes from dog pancreas containing signal peptidase activity. Proc. Natl. Acad. Sci. USA *74*, 5598-5602.
James, P., Halladay, J., and Craig, E.A. (1996). Genomic libraries and a host strain designed for highly efficient two-hybrid selection in yeast. Genetics *144*, 1425-1436.
Jauvion, V., Elmayan, T., and Vaucheret, H. (2010). The conserved RNA trafficking proteins HPR1 and TEX1 are involved in the production of endogenous and exogenous small interfering RNA in *Arabidopsis*. Plant Cell *22*, 2697-2709.
John, D.C., and Bulleid, N.J. (1994). Prolyl 4-hydroxylase: defective assembly of alpha-subunit mutants indicates that assembled alpha-subunits are intramolecularly disulfide bonded. Biochemistry *33*, 14018-14025.
Jones, A.M., and Herman, E.M. (1993). A K-D-E-L-containing auxin-binding protein is located at the plasma membrane and within the cell wall. Plant Physiol. *101*, 595-606.
Kanai, S., Toh, H., Hayano, T., and Kikuchi, M. (1998). Molecular evolution of the domain structures of protein disulfide isomerases. J. Mol. Evol. *47*, 200-210.
Karniely, S., and Pines, O. (2005). Single translation-dual destination: mechanisms of dual protein targeting in eukaryotes. EMBO Rep. *6*, 420-425.
Kerk, D., Bulgrien, J., Smith, D.W., and Gribskov, M. (2003). *Arabidopsis* proteins containing similarity to the universal stress protein domain of bacteria. Plant Physiol. *131*, 1209-1219.
Kim, J.M., and Mayfield, S.P. (1997). Protein disulfide isomerase as a regulator of chloroplast translational activation. Science *278*, 1954-1957.
Kong, Z., Li, M., Yang, W., Xu, W., and Xue, Y. (2006). A novel nuclear-localized CCCH-type zinc finger protein, OsDOS, is involved in delaying leaf senescence in rice. Plant Physiol. *141*, 1376-1388.
Lahav, J., Gofer-Dadosh, N., Luboshitz, J., Hess, O., and Shaklai, M. (2000). Protein disulfide isomerase mediates integrin-dependent adhesion. FEBS Lett. *475*, 89-92.
Lamberg, A., Jauhiainen, M., Metso, J., Ehnholm, C., Shoulders, C., Scott, J., Pihlajaniemi, T., and Kivirikko, K.I. (1996). The role of protein disulphide isomerase in the microsomal triacylglycerol transfer protein does not reside in its isomerase activity. Biochem. J. *315*, 533-536.
Lange, A., Mills, R.E., Lange, C.J., Stewart, M., Devine, S.E., and Corbett, A.H. (2007). Classical nuclear localization signals: definition, function, and interaction with importin alpha. J. Biol. Chem. *282*, 5101-5105.
Lappi, A.K., Lensink, M.F., Alanen, H.I., Salo, K.E., Lobell, M., Juffer, A.H., and Ruddock, L.W. (2004). A conserved arginine plays a role in the catalytic cycle of the protein disulphide isomerases. J. Mol. Biol. *335*, 283-295.
Lee, S.-O., Cho, K., Cho, S., Kim, I., Oh, C., and Ahn, K. (2010). Protein disulphide isomerase is required for signal peptide peptidase-mediated protein degradation. EMBO J. *29*, 363-375.
Levitan, A., Trebitsh, T., Kiss, V., Pereg, Y., Dangoor, I., and Danon, A. (2005). Dual targeting of the protein disulfide isomerase RB60 to the chloroplast and the endoplasmic reticulum. Proc. Natl. Acad. Sci. USA *102*, 6225-6230.
Li, C.P., and Larkins, B.A. (1996). Expression of protein disulfide isomerase is elevated in the endosperm of the maize floury 2 mutant. Plant Mol. Biol. *30*, 873-882.
Lu, D.-P., and Christopher, D.A. (2006). Immunolocalization of a protein disulfide isomerase to *Arabidopsis thaliana* chloroplasts and its association with starch biogenesis. Int. J. Plant Sci. *167*, 1-9.
Lu, D.-P., and Christopher, D.A. (2008). Endoplasmic reticulum stress activates the expression of a sub-group of protein disulfide isomerase genes and AtbZIP60 modulates the response in *Arabidopsis thaliana*. Mol. Genet. Genomics *280*, 199-210.
Lucero, H.A., and Kaminer, B. (1999). The role of calcium on the activity of ER calcistorin/Protein-disulfide Isomerase and the significance of the C-terminal and itscalcium binding A comparison with mammalian protein-disulfide isomerase. J. Biol. Chem. *274*, 3243-3251.
Lumb, R.A., and Bulleid, N.J. (2002). Is protein disulfide isomerase a redox-dependent molecular chaperone? EMBO J. *21*, 6763-6770.
Markus, M., and Benezra, R. (1999). Two isoforms of protein disulfide isomerase alter the dimerization status of E2A proteins by a redox mechanism. J. Biol. Chem. *274*, 1040-1049.
Maruyama, D., Endo, T., and Nishikawa, S. (2010). BiP-mediated polar nuclei fusion is essential for the regulation of endosperm nuclei proliferation in *Arabidopsis thaliana*. Proc. Natl. Acad. Sci. USA *107*, 1684-1689.
Mayer, M., Kies, U., Kammermeier, R., and Buchner, J. (2000). BiP and PDI cooperate in the oxidative folding of antibodies *in vitro*. J. Biol. Chem. *275*, 29421-29425.
Motohashi, K., Kondoh, A., Stumpp, M.T., and Hisabori, T. (2001). Comprehensive survey of proteins targeted by chloroplast thioredoxin. Proc. Natl. Acad. Sci. USA *98*, 11224-11229.
Nelson, B.K., Cai, X., and Nebenführ, A. (2007). A multicolored set of *in vivo* organelle markers for co-localization studies in *Arabidopsis* and other plants. Plant J. *51*, 1126-1136.
Neuteboom, L.W., Matsumoto, K.O., and Christopher, D.A. (2009). An extended AE-rich N-terminal trunk in secreted pineapple cystatin enhances inhibition of fruit bromelain and is post-translationally removed during ripening. Plant Physiol. *151*, 515-527.
Ohtani, H., Wakui, H., Ishino, T., Komatsuda, A., and Miura, A.B. (1993). An isoform of protein disulfide isomerase is expressed in the developing acrosome of spermatids during rat spermiogenesis and is transported into the nucleus of mature spermatids and epididymal spermatozoa. Histochemistry *100*, 423-429.
Okita, T.W., and Rogers, J.C. (1996). Compartmentation of proteins in the endomembrane system of plant cells. Annu. Rev. Plant. Physiol. Plant Mol. Biol. *47*, 327-350.
Onda, Y., Nagamine, A., Sakurai, M., Kumamaru, T., Ogawa, M., and Kawagoe, Y. (2011). Distinct roles of protein disulfide isomerase and p5 sulfhydryl oxidoreductases in multiple pathways for oxidation of structurally diverse storage proteins in rice. Plant Cell *23*, 210-223.
Ondzighi, C.A., Christopher, D.A., Cho, E.J., Chang, S.C., and Staehelin, L.A. (2008). *Arabidopsis* protein disulfide isomerase-5 inhibits cysteine proteases during trafficking to vacuoles before programmed cell death of the endothelium in developing seeds. Plant Cell *20*, 2205-2220.
Ostermeier, M., De Sutter, K., and Georgiou, G. (1996). Eukaryotic protein disulfide isomerase complements *E. coli dsbA* mutants and increases the yield of heterologous secreted protein with disulfide bonds. J. Biol. Chem. *271*, 10616-10622.
Pagnussat, G.C., Yu, H.J., Ngo, Q.A., Rajani, S., Mayalagu, S., Johnson, C.S., Capron, A., Xie, L.F., Ye, D., and Sundaresan, V. (2005). Genetic and molecular identification of genes required for female gametophyte development and function in *Arabidopsis*. Development *132*, 603-614.
Plath, K., Mothes, W., Wilkinson, B.M., Stirling, C.J., and Rapoport, T.A. (1998). Signal sequence recognition in posttranslational protein transport across the yeast ER membrane. Cell *94*, 795-807.
Pomeranz, M.C., Hah, C., Lin, P.-C., Kang, S.G., Finer, J.J., Blackshear, P.J., and Jang, J.C. (2010). The *Arabidopsis* tandem zinc finger protein AtTZF1 traffics between the nucleus and cytoplasmic foci and binds both DNA and RNA. Plant Physiol. *152*, 151-165.
Powers, T., and Walter, P. (1996). The nascent polypeptide-associated complex modulates interactions between the signal recognition particle and the ribosome. Curr. Biol. *6*, 331-338.
Rapoport, T.A., Matlack, K.E., Plath, K., Misselwitz, B., and Staeck, O. (1999). Posttranslational protein translocation across the membrane of the endoplasmic reticulum. Biol. Chem. *380*, 1143-1150.
Rigobello, M.P., Donella-Deana, A., Cesaro, L., and Bindoli, A. (2001). Distribution of protein disulphide isomerase in rat liver

mitochondria. Biochem. J. *356*, 567-570.
Rosenthal, J.A., Chen, H., Slepnev, V.I., Pellegrini, L., Salcini, A.E., Di Fiore, P.P., and De Camilli, P. (1999). The epsins define a family of proteins that interact with components of the clathrin coat and contain a new protein module. J. Biol. Chem. *274*, 33959-33965.
Rout, M.P., Aitchison, J.D., Magnasco, M.O., and Chait, B.T. (2003). Virtual gating and nuclear transport: the hole picture. Trends Cell Biol. *13*, 622-628.
Shimada, H., Mochizuki, M., Ogura, K., Froehlich, J.E., Osteryoung, K.W., Shirano, Y., Shibata, D., Masuda, S., Mori, K., and Takamiya, K. (2007). *Arabidopsis* cotyledon-specific chloroplast biogenesis factor CYO1 is a protein disulfide isomerase. Plant Cell *19*, 3157-3169.
Shimoni, Y., Zhu, X.Z., Levanony, H., Segal, G., and Galili, G. (1995). Purification characterization and intracellular localization of glycosylated protein disulfide isomerase from wheat grains. Plant Physiol. *108*, 327-335.
Sone, M., Kishigami, S., Yoshihisa, T., and Ito, K. (1997). Roles of disulfide bonds in bacterial alkaline phosphatase. J. Biol. Chem. *272*, 6174-6178.
Stockton, J.D., Merkert, M.C., and Kellaris, K.V. (2003). A complex of chaperones and disulfide isomerases occludes the cytosolic face of the translocation protein Sec61p and affects translocation of the prion protein. Biochemistry *42*, 12821-12834.
Swanson, R., Locher, M., and Hochstrasser, M. (2001). A conserved ubiquitin ligase of the nuclear envelope/endoplasmic reticulum that functions in both ER-associated and matalpha2 repressor degradation. Genes Dev. *15*, 2660-2674.
Takemoto, Y., Coughlan, S.J., Okita, T.W., Satoh, H., Ogawa, M., and Kumamaru, T. (2002). The rice mutant esp2 greatly accumulates the glutelin precursor and deletes the protein disulfide isomerase. Plant Physiol. *128*, 1212-1222.
Tamura, K., Yamada, K., Shimada, T., and Hara-Nishimura, I. (2004). Endoplasmic reticulum-resident proteins are constitutively transported to vacuoles for degradation. Plant J. *39*, 393-402.
Tu, B., Ho-Schleyer, S.C., Travers, K.J., and Weissman, K.J. (2000). Biochemical basis of oxidative protein folding in the endoplasmic reticulum. Science *290*, 1571-1574.
Turano, C., Coppari, S., Altieri, F., and Ferraro, A. (2002). Proteins of the PDI family: unpredicted non-ER locations and functions. J. Cell. Physiol. *193*, 154-163.
Wang, H., Boavida, L.C., Ron, M., and McCormick, S. (2008). Truncation of a protein disulfide isomerase, PDIL2-1, delays embryo sac maturation and disrupts pollen tube guidance in *Arabidopsis thaliana*. Plant Cell *20*, 3300-3311.
Wilson, R., Lees, J.F., and Bulleid, N.J. (1998). Protein disulfide isomerase acts as a molecular chaperone during the assembly of procollagen. J. Biol. Chem. *273*, 9637-9643.
Wu, F.H., Shen, S.C., Lee, L.Y., Lee, S.H., Chan, M.T., and Lin, C. -S. (2009). Tape-*Arabidopsis* sandwich - a simpler *Arabidopsis* protoplast isolation method. Plant Methods *5*, 1-10.
Xu, P., Radena, D., Doyle, III F.J., and Robinson, A.S. (2005). Analysis of unfolded protein response during single-chain antibody expression in *Saccaromyces cerevisiae* reveals different roles for BiP and PDI in folding. Metab. Eng. *7*, 269-279.
Yoo, S.D., Cho, Y.H., and Sheen, J. (2007). *Arabidopsis* mesophyll protoplasts: a versatile cell system for transient gene expression analysis. Nat. Protoc. *2*, 1565-1572.
Yoshimori, T., Semba, T., Takemoto, H., Akagi, S., Yamamoto, A., and Tashiro, Y. (1990). Protein disulfide-isomerase in rat exocrine pancreatic cells is exported from the endoplasmic reticulum despite possessing the retention signal. J. Biol. Chem. *265*, 15984-15990.
Zaltsman, A., Yi, B.Y., Gafni, Y., and Citovsky, V. (2007). Yeast-plant coupled vector system for identification of nuclear proteins. Plant Physiol. *145*, 1264-1271.